

UNCLASSIFIED

AD NUMBER

ADB007095

LIMITATION CHANGES

TO:

Approved for public release; distribution is unlimited.

FROM:

Distribution authorized to U.S. Gov't. agencies only; Test and Evaluation; NOV 1972. Other requests shall be referred to Air Force Flight Test Center, Edwards AFB, CA.

AUTHORITY

AFFTC ltr 2 Mar 1976

THIS PAGE IS UNCLASSIFIED

ADB007095

AD
DDC
FILE
COPY,
C

18

2

FTC-TD-73-4

See 1473



DETERMINING THE PERFORMANCE ENVELOPES OF SHORT RANGE MISSILES

THOMAS P. MCATEE
Major, USAF

TECHNOLOGY DOCUMENT NO. 73-4
NOVEMBER 1973

Distribution limited to U.S. Government agencies only
(Test and Evaluation), August 1973. Other requests
for this document must be referred to AFFTC/DOFC,
Edwards AFB, California 93523.

DDC
RECEIVED
OCT 21 1973
D

AIR FORCE FLIGHT TEST CENTER
EDWARDS AIR FORCE BASE, CALIFORNIA
AIR FORCE SYSTEMS COMMAND
UNITED STATES AIR FORCE

AD NO.

APPROVED BY	
DDC	With Section <input type="checkbox"/>
DDC	With Section <input checked="" type="checkbox"/>
UNCLASSIFIED	<input type="checkbox"/>
JUSTIFICATION	
BY	
DISTRIBUTION/AVAILABILITY CODES	
DDC	AVAIL. CODE/W SPECIAL
B	

Qualified requesters may obtain copies of this report from the Defense Documentation Center, Cameron Station, Alexandria, Va. Department of Defense contractors must be established for DDC services, or have "need to know" certified by cognizant military agency of their project or contract.

DDC release to OTS is not authorized

When US Government drawings, specifications, or other data are used for any purpose other than a definitely related government procurement operation, the government thereby incurs no responsibility nor any obligation whatsoever; and the fact that the government may have formulated, furnished, or in anyway supplied the said drawings, specifications, or any other data is not to be regarded by implication or otherwise, as in any manner licensing the holder or any other person or corporation or conveying any rights or permission to manufacture, use or sell any patented invention that may in any way be related thereto.

Do not return this copy, Retain or destroy

FTC-TD-73-4

**DETERMINING THE
PERFORMANCE ENVELOPES OF
SHORT RANGE MISSILES**

THOMAS P. MCATEE
Major, USAF

Distribution limited to U.S. Government agencies only
(Test and Evaluation), August 1973. Other requests
for this document must be referred to AFFTC/DOFC,
Edwards AFB, California 93523.

DDC
RECEIVED
OCT 21 1975
RECEIVED
D


FOREWORD

This technology document is the result of studies performed at Holloman AFB, New Mexico, and Edwards AFB, California, between February 1969 and November 1972. It was motivated by the rather poor success rate in envelope determination of short range missiles such as the AIM-4H, AIM-9E, and Redeye Air-Launched Missile (RAM) at Holloman AFB from 1966 to 1969. Although the need for new and better test methods was apparent in 1969, funds were not available, and the study was performed on an individual "extra-curricular" basis. It was not until the author was transferred to Edwards AFB as an instructor at the USAF Test Pilot School, that the means were available to complete the study and publish this report. The material presented here was originally developed as a course in Short Range Missile Testing to be presented during the Systems Testing phase of the Test Pilot School curriculum.

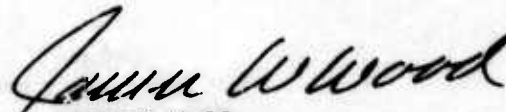
The author would like to acknowledge the contributions of Colonel Joseph A. Guthrie, Commandant of the USAF Test Pilot School, who provided the support necessary to complete the study and publish this document.

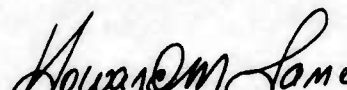
Foreign announcement and dissemination by the Defense Documentation Center are not authorized because of technology restrictions of the U.S. Export Controls Act as implemented by AFR 400-10.

Prepared by :


THOMAS P. McATEE
Major, USAF

Reviewed and approved by :
7 September 1973


JAMES W. WOOD
Colonel, USAF
Deputy Commander for Operations


HOWARD M. LANE
Brigadier General, USAF
Commander

ABSTRACT

This report presents the results of a study to develop a reliable test method for determining a short range missile's performance envelope. Three main areas are covered: (1) drone control, (2) derivation of a computer program for predicting flightpath relationships, and (3) a new test technique that when properly applied will guarantee that the missile is launched on the edge of its envelope. This technique is unique in that it allows the missile to be fired at a number of acceptable launch conditions and uses real time computation to determine when an acceptable launch condition exists. Application of this method is simple and inexpensive. Added to this, its inherent reliability will allow test agencies to accurately determine a missile's performance envelope and will result in substantial savings by greatly reducing the number of required missile launches for envelope determination.

table of contents

	Page No.
LIST OF ILLUSTRATIONS	v
LIST OF ABBREVIATIONS AND SYMBOLS	vi-viii
INTRODUCTION	1
Background	1
Objective	1
The Missile Performance Envelope	1
The Problem	2
The Solution	3
CHAPTER I - TARGET DRONE CONTROL	5
History	7
The Improved Maneuverability Kit	7
Advanced Increased Maneuverability	10
CHAPTER II - FLIGHTPATH PREDICTION (FLIGHT PLANNING)	13
Objective	15
The Maneuver	15
Attack Situation	16
Target Flightpath Variables	17
Determination of V_T	18
Determination of ω_T	20
Expansion to Three Dimensions	23
Launcher Flightpath Variables	24
Determination of V_L	24
Determination of ϕ and α	25
Determination of n_L	26
Summary	28
State Equations	29
Control and Related Equations	29
CHAPTER III - TEST TECHNIQUES	31
Background	32
Objective	32
Acceptable Launch Conditions	32
Selecting Alternate Launch Points	33
Real Time Flightpath Computation	36
The "Fire" Signal	37
Launcher and Target Velocities	39
Summary	39
APPENDIX I - COMPUTER PROGRAM AND SAMPLE COMPUTER OUTPUT	41
REFERENCES	47

list of Illustrations

<u>Figure No.</u>	<u>Title</u>	<u>Page No.</u>
1	Typical Missile Performance Envelope _____	2
2	Lateral Axis of BQM-34A with IMK _____	7
3	Longitudinal Axis of the BQM-34A with IMK _____	8
4	Typical IMK Variables for a 4-g Turn _____	9
5	Longitudinal Axis of the AIM Mode _____	10
6	Lateral Axis of the AIM Mode _____	11
7	Drone Variables for 6-g Turn with the AIM Mode _____	12
8	Attack Situation _____	17
9	An Aircraft in a Level Turn _____	20
10	An Aircraft in a Bank _____	21
11	Three-Dimensional View of an Attack Situation _____	23
12	Flightpath Prediction Curves _____	28
13	Construction of an Acceptable Launch Parameter Matrix _____	34
14	Matrix of Acceptable Launch Conditions _____	35
15	Real Time Computation of Flightpath Parameters _____	36
16	Flow Diagram for Comparison of Predicted Param- eters with Acceptable Conditions _____	38

LIST OF ABBREVIATIONS AND SYMBOLS

<u>Item</u>	<u>Definition</u>
AIM	Advanced Increased Maneuverability
AR	launcher aspect ratio
AR_T	aspect ratio of the target
C_{D0}	zero lift coefficient of drag of the launcher
C_{D0T}	zero lift drag coefficient of the target
C.F.	centripetal force (ft-lb)
C_L	lift coefficient of the launcher
C_{LT}	lift coefficient of the target.
D	drag of the launcher (lb)
D_0	drag at $t=0$ for the launcher
e	Oswald's efficiency factor of the launcher
e_T	Oswald's efficiency factor of the target
g	acceleration of gravity, 32.2 ft/sec ²
h	altitude (ft)
h_c	commanded altitude, drone autopilot (ft)
IMK	Increased Maneuverability Kit
L	lift
m	mass (slugs)
n	load factor (g)
n_c	commanded g, drone autopilot
n_L	launcher load factor
n_T	target load factor
R	range (ft)
R_m	measured range (ft)
R_p	predicted range
RT	radius of turn (ft)
S	wing area of the launcher (ft)

<u>Item</u>	<u>Definition</u>
S_T	wing area of the target
T	thrust of the launcher (lb)
TCA	track crossing angle. The angle between the true velocity vectors of the launcher and the target
T_T	target thrust (lb)
V_L	launcher true velocity (KTAS)
V_{L0}	launcher velocity of $t=0$ or launcher trim velocity for determining thrust
V_T	target true velocity (KTAS)
V_{VL}	vertical velocity of the launcher
W	weight of the launcher (lb)
W_T	target weight
Z	vertical distance between the target and the launcher (ft)
α	angle of attack of the launcher (deg)
δ	sight depression angle (deg)
δ_a	aileron deflection (deg)
δ_e	elevator deflection (deg)
ϵ_h	altitude error (ft)
ϵ_n	load factor error, drone autopilot
ϵ_ϕ	bank angle error (deg)
θ	track crossing angle (deg)
θ_P	predicted track crossing angle (deg)
λ_L	angle between launcher velocity vector and line of sight vector (deg)
λ_T	angle between target velocity vector and line of sight vector (deg)
λ_V	angle between line of sight and the horizontal plane adjacent to the launcher (deg)
ρ	air density

<u>Item</u>	<u>Definition</u>
τ	time constant for target g profile
ϕ	bank angle (deg)
ϕ_C	commanded bank angle, drone autopilot (deg)
ϕ_L	bank angle of the launcher (deg)
ϕ_T	bank angle of the target
ω	angular rate of velocity vector or "rate of turn"
ω_L	angular rate of launcher velocity vector
ω_R	angular rate of line of sight vector
ω_T	angular rate of target velocity vector

INTRODUCTION

BACKGROUND

During the mid-1960's a great deal of money was spent on designing and testing lightweight, highly maneuverable air-to-air missiles that could be used in a "hassling" situation. The requirement for such a missile became obvious in the early stages of the air war over North Vietnam; when time after time American pilots found themselves unable to use traditional long range interceptor tactics. What usually prevailed was a close-in "dog fight" type of encounter. Unfortunately, our missiles had been designed for the interceptor role, and when faced with these new tactics they proved to be inadequate. As a result, specifications were laid down for a missile that could be fired successfully against a "high g" maneuvering target from extremely short ranges. For some situations these ranges were less than 1,500 feet. As a result, the term "Short Range Missile" was coined.

Many difficulties were encountered when these weapons were tested. Missile characteristics such as separation from the launch aircraft at high angles of attack, guidance and warhead arming, missile stability, etc., became extremely critical at these short ranges. Determination of these characteristics through flight test posed some unique problems. The most perplexing problem for the test forces, however, was the verification of the missile's performance envelope. This, unfortunately, was the most important objective of the test programs. The lack of success in this area motivated several studies. The results of one of those studies are presented in this paper.

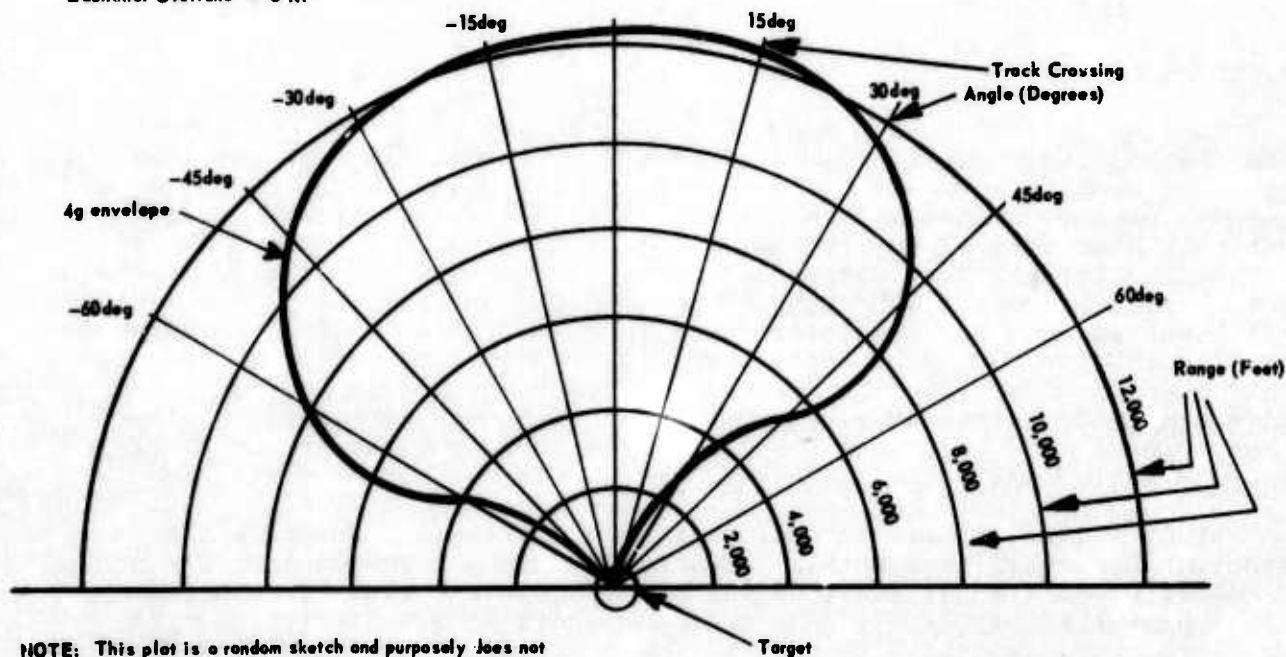
OBJECTIVE

The purpose of this paper, is to define a test method for determining a short range missile's performance (or firing) envelope. The methods presented here are new. They have never been used in actual missile tests. They are based, however, on experience gained from previous tests, and should guarantee a substantial increase in success rates for future tests.

THE MISSILE PERFORMANCE ENVELOPE

Figure 1 presents a typical missile performance envelope. The graph represents all the combinations of range and track crossing angle that could occur in an air-to-air hassle (track crossing angle or "TCA" is the relative angle between the velocity vectors of the target and the launcher). The envelope, defined by the solid black line, specifies the limits of range and TCA at which the missile can be fired and still hit the target. These curves are derived on the assumption that target "g" remains constant from launch throughout the missile's flight. If the target "g" is increased, the envelope will shrink. If it is decreased, the envelope will expand. The altitude and Mach number of the target and launcher are also specified for each plot. Additional plots are required for each set of specified conditions.

Altitude - 20,000 Feet
 Target Mach Number - .8
 Target Load Factor - 4g's
 Launcher Overtake - 0 Kt



NOTE: This plot is a random sketch and purposely does not represent any known missile performance envelope.

Figure 1 Typical Missile Performance Envelope

Notice that the envelope is not symmetrical about the zero TCA line. This results from the fact that it is easier for the missile to maneuver against a target that is turning towards the launcher's flightpath rather than away from it. Be careful. This plot does not display a horizontal situation. It is solely a plot of acceptable launch conditions (i.e., range and TCA).

Ordinarily, the missile contractor is required to submit plots of the predicted performance envelope. These predictions are usually based on data obtained from computer simulations and wind tunnel tests. It is the job of the test force to determine if these predictions are correct. To do this the test force must find a way to launch the missile at conditions that fall exactly on the edge of the predicted envelope. Barring any malfunction, the verification of the performance envelope can then be made against "hit or miss" criteria.

THE PROBLEM

The problem is to maneuver the target and the launcher so that they arrive at an acceptable set of launch conditions. Acceptable launch conditions are those that fall on the edge of the contractor's predicted performance envelope. The critical parameters to be obtained at launch are:

1. Target load factor
2. Range
3. TCA
4. Target and launcher Mach numbers

Altitude is not considered critical due to the relative ease of maintaining the aim altitude.

To solve the problem, the launcher pilot and the target drone operator must satisfy a particular set of these parameters simultaneously. This is no simple task. Those who have had success during long range missile tests can easily be led down the primrose path. There are several advantages with long range missile testing. For one, ground-based radar can be used to help vector the pilot into a proper set of launch conditions prior to turning the target drone. Due to the relatively long missile flight, the effect of this is negligible. For another, percentage-wise, a 200-foot error at 6 miles is negligible, while at 2,000 feet it is substantial.

When test forces were first presented with this problem, a variety of solutions was proposed, some of them bordering on the ridiculous. Most of the test methods used could best be described as "black art", and usually gave very poor results. Probably the most successful method was the "Kentucky windage" method, in which the pilot merely eyeballed the situation and fired when it looked right. The key word in planning a test was redundancy. In other words, if enough missiles were planned to be fired at the same test point, sooner or later, one would hopefully be fired at the desired parameters. The amount of money required for this approach was quite often unacceptable and many programs were either scrapped or performance envelopes were never accurately determined.

THE SOLUTION

In order to solve this problem there are three main areas to consider:

1. Control of the target drone - target load factor is one of the primary parameters. Therefore, a constant, predictable and relatively accurate "g" profile is imperative (Chapter I).
2. Flightpath prediction (Flight Planning) - The pilot should have a means of pre-planning his attack maneuver. In other words, he should be able to determine at what range, speed and throttle setting he should start in order to arrive at the desired launch conditions. Planning charts must therefore be provided. This can be done through computer simulation with flight test verification (Chapter II).
3. Test techniques - A test technique must be developed that insures that the missile is launched on the edge of the envelope (Chapter III).

THIS PAGE LEFT BLANK FOR PRESENTATION PURPOSES

CHAPTER I

TARGET DRONE CONTROL

THIS PAGE LEFT BLANK FOR PRESENTATION PURPOSES

HISTORY

The BQM-34A is the primary target drone used for subsonic air-to-air missile testing. It is probably the most modified airframe in the world today. Initially, it was designed and built as an inexpensive, fast moving target for testing ground-launched anti-aircraft missiles. As needs increased, various changes were made to enable the drone to perform one job or another that the original design had never called for. Regardless of the change, money was always a major consideration, so design was quite often based on what could be done within a certain price range. As a result, the early BQM-34A's were extremely limited in what they could do. In the mid-1960's, the BQM-34A incorporated a modified control system known as the Increased Maneuverability Kit (IMK). This gave the drone the ability to maneuver at load factors up to 4 g's. However, due to the mechanization of the system, the drone could not hold a constant g, nor was the g profile predictable or repeatable (the g profile is the time history of g's throughout the maneuver). In order to better understand what is required for good drone control, the mechanization of the IMK and its inherent problems should be studied.

THE IMPROVED MANEUVERABILITY KIT

The IMK is a two-axis control system (ailerons and elevator) with a ground-controlled aileron trim capability. An autopilot controls the ailerons and elevator to hold a level constant bank turn. When a turn is commanded, the autopilot uses the ailerons to roll the drone to a preplanned bank angle and hold that bank angle throughout the maneuver (figures 2 and 3 demonstrate the design concept of the IMK. They are not necessarily identical to the actual design).

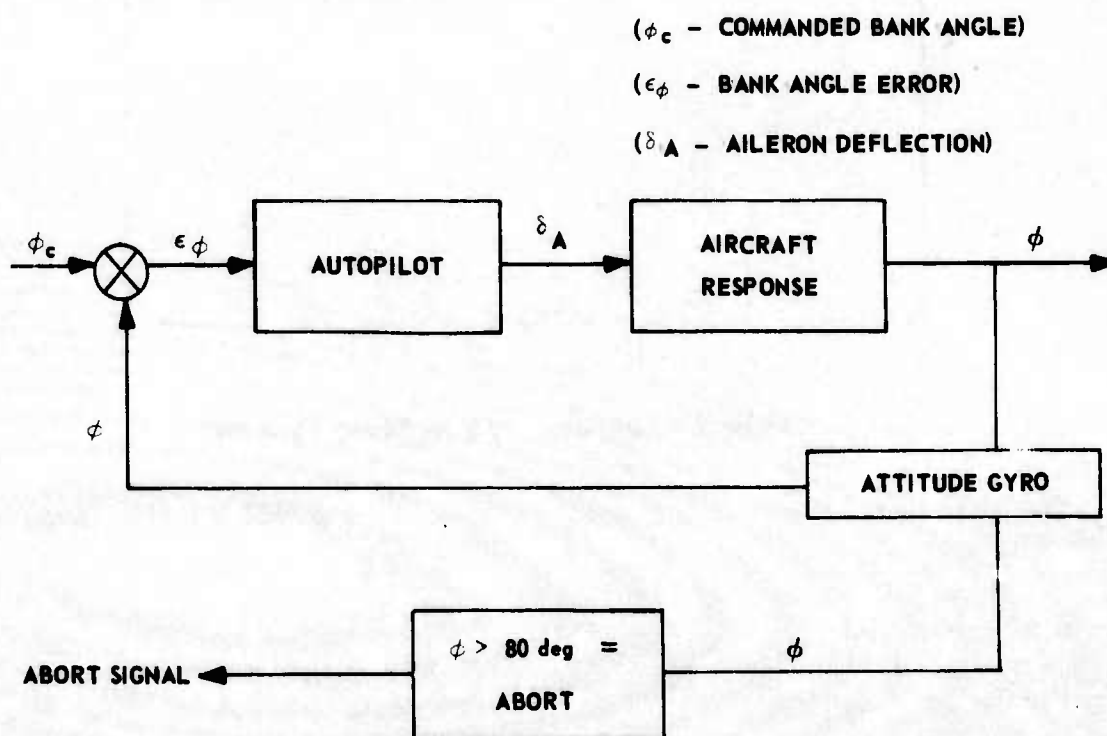


Figure 2 Lateral Axis of BQM-34A With IMK

The autopilot controls the elevator to hold a constant altitude. During the roll into the turn, a pre-set ramp input is fed to the elevator to compensate for a lag in the altitude sensing. (This rarely works properly so the drone usually has an initial rate of climb.) Once the bank angle is established, the elevator is then used to fly to and maintain the altitude that was measured at the initiation of the turn (figure 3). The "g" profile therefore is largely a function of the oscillations about the aim altitude. As a result, the turn rate is random and unrepeatable.

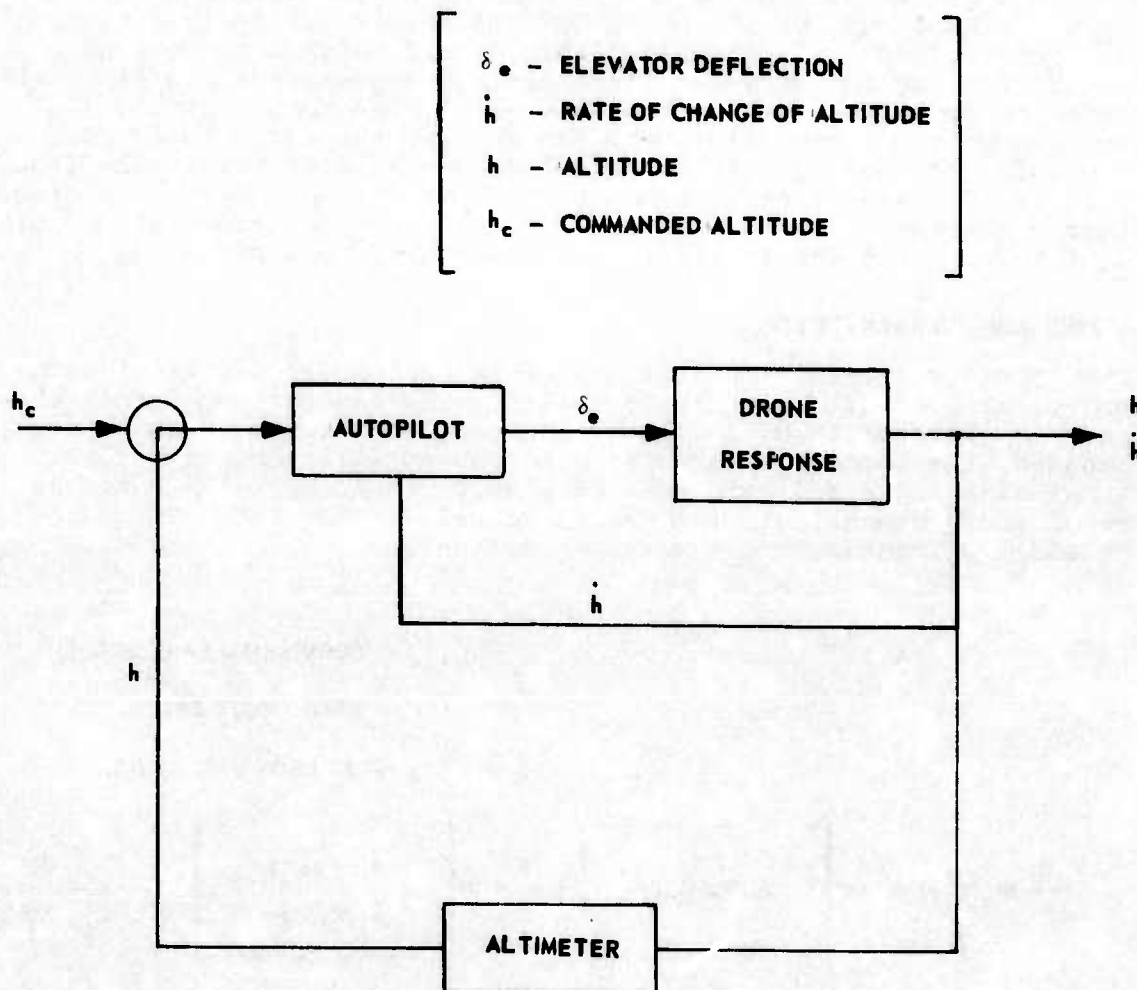


Figure 3 Longitudinal Axis of the BQM-34A with IMK

The philosophy behind the control system is based on the level flight relation,

$$n = \frac{1}{\cos \phi}$$

where: n = load factor

ϕ = bank angle

Since the load factor is a function of ϕ alone, by selecting a particular bank angle, a corresponding load factor should result. For example, if a load factor of 2 is desired, a bank angle of 60 degrees is set into the autopilot. As was mentioned before, this setting is preselected on the ground and cannot be changed in flight. Therefore, the drone operator cannot vary the bank angle directly to try to change the g profile. But all is not lost. The operator can vary the load factor with aileron trim. With the IMK the controller is able to vary bank angle ± 10 degrees with aileron trim. This in turn will cause a descent or climb. Sensing this, the autopilot will increase or decrease the load factor to return the drone to the reference altitude. This technique is used extensively; however, precise g control is still impossible due to the long time lag between input and response. Added to this, the drone controller must be extremely careful when he uses this technique, since the autopilot will automatically abort the maneuver and level the wings if the bank angle exceeds 80 degrees. A typical g profile with this system can be seen in figure 4.

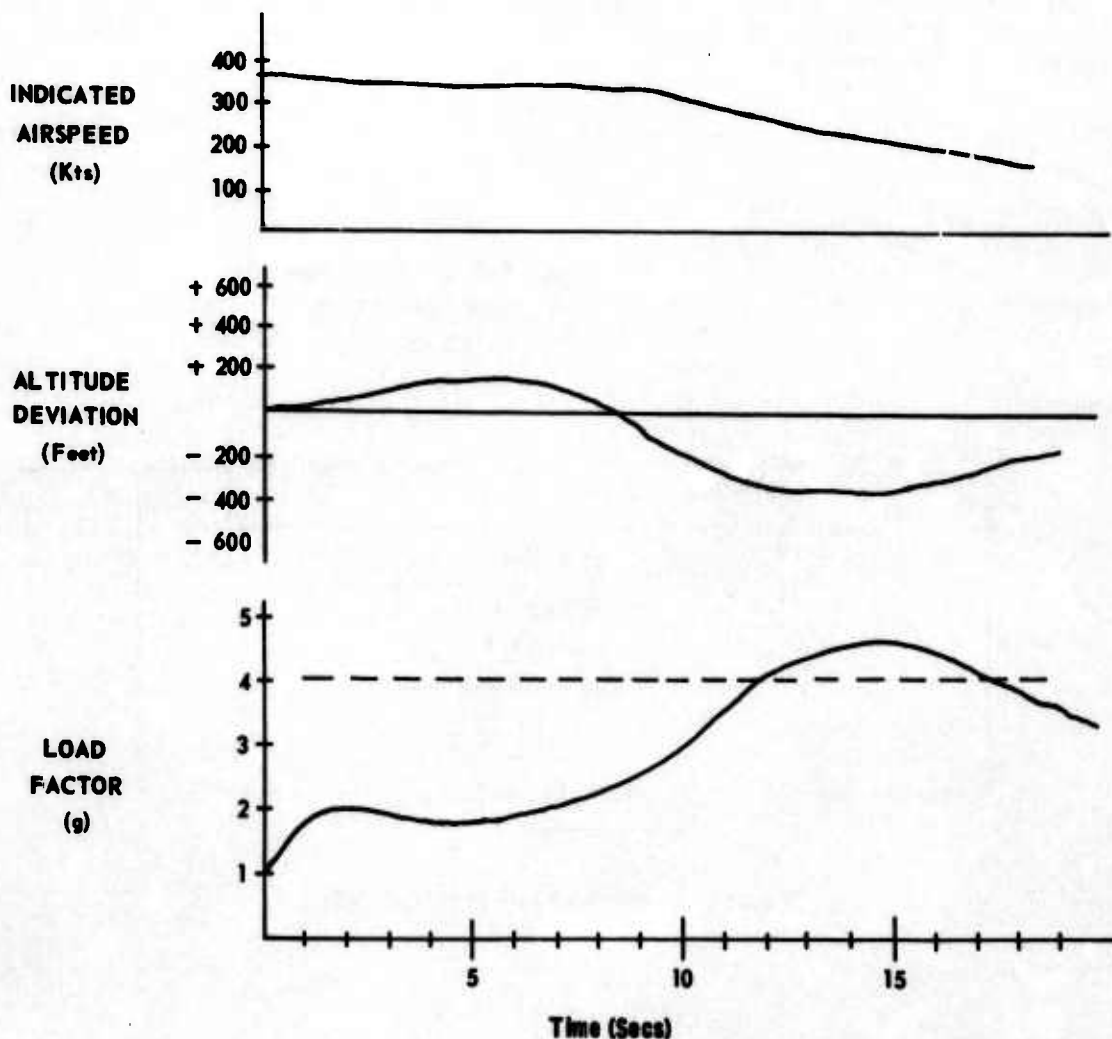


Figure 4 Typical IMK Variables For a 4-g Turn

Although altitude is usually maintained fairly well, the g profile makes it nearly impossible to arrive at any set of preselected launch parameters. It became obvious during the short range missile tests that the first step in solving the problem was to build a drone control system that could fly a constant g profile that is predictable and repeatable. It should also be able to maintain altitude reasonably well.

ADVANCED INCREASED MANEUVERABILITY

In 1969, a contract was let to Lear-Siegler, Inc., to design and build such a system. It was referred to as the Advanced Increased Maneuverability (AIM) mode, and was part of the "Versatile Automatic Flight Control System". The mechanization of the AIM mode provides for much more precise control of load factor. This is done by using the elevator to control the g's while bank angle is used to control altitude. A simplified block diagram of the longitudinal and lateral control axes are presented in figures 5 and 6.

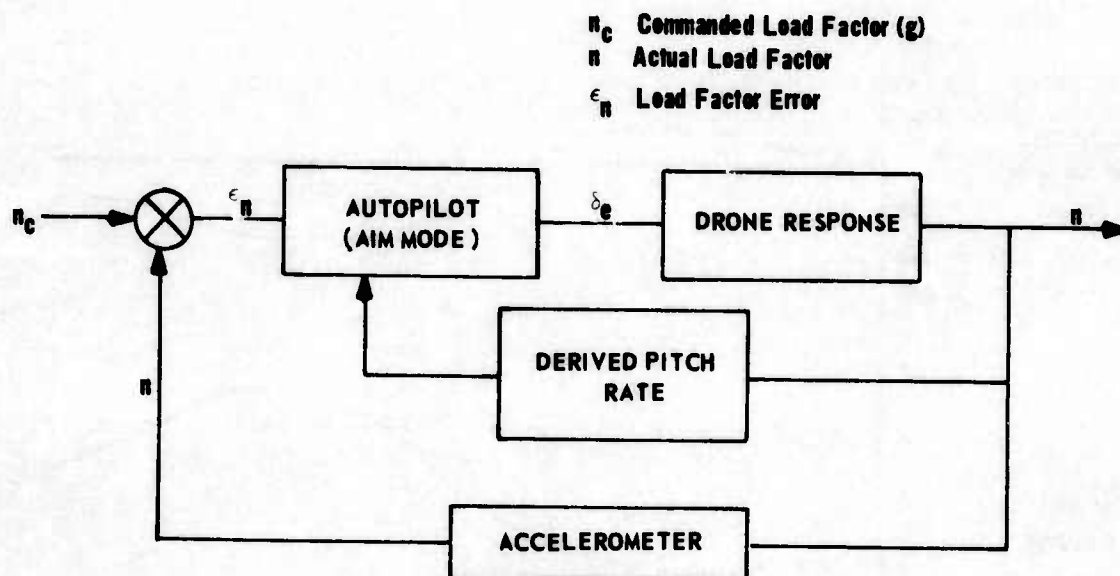


Figure 5 Longitudinal Axis of the AIM Mode

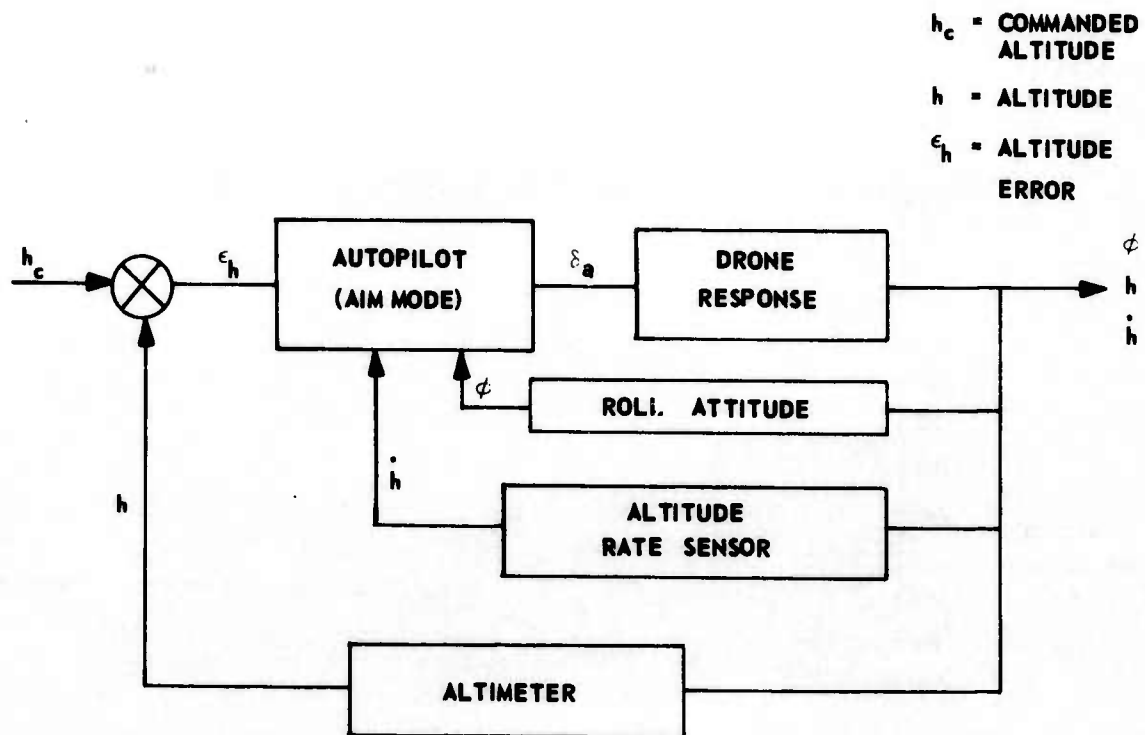


Figure 6 Lateral Axis of the AIM Mode

In the AIM mode the elevator position is dependent upon normal acceleration, i.e., the autopilot positions the elevator so as to hold a desired load factor. It is easy to see how this mechanization allows for extremely precise control of load factor.

The bank angle is dependent upon altitude error and the rate of change of altitude. That is, if the drone is low, the autopilot will decrease the bank angle causing the drone to climb. As the drone approaches the aim altitude the autopilot increases bank angle to reduce rate of climb so that it is approximately zero when the drone reaches its aim altitude.

Although this may seem confusing, it is similar to the way a pilot controls an airplane in a level turn. The validity of this approach was proven during flight tests performed on the AIM mode at Holloman AFB during 1971 and 1972 (reference 1). The results of these tests showed that precise g control was possible and that the altitude error could be maintained within reasonable limits. Figure 7 shows a typical plot of the significant variables during a 6-g AIM turn.

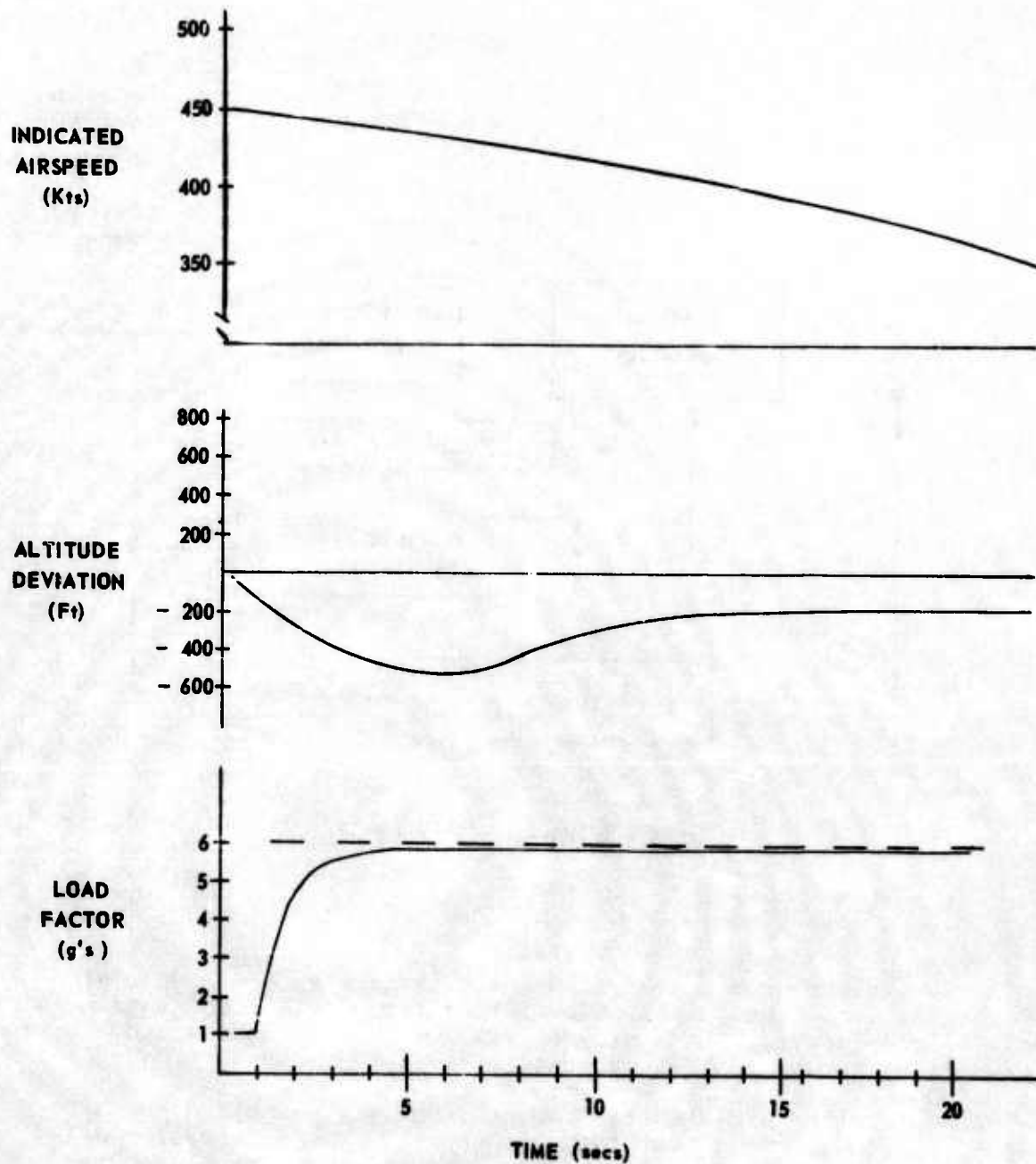


Figure 7 Drone Variables for 6-g Turn With AIM Mode

Although there are still certain limits on the system and various problems arise with "bent birds", the system does fly with predictability and repeatability. Refinements to the system will continue to be made, but the first step in solving the problem is essentially done.

CHAPTER II
FLIGHTPATH PREDICTION
'FLIGHT PLANNING'

THIS PAGE LEFT BLANK FOR PRESENTATION PURPOSES

The second step is to derive a set of plots that a pilot can use to help him plan his attack. He will be given a set of desired launch parameters (i.e., target g, range and TCA). To reach those parameters, he must know where to start and how to fly the attack maneuver. Actual flight test time is at a premium since it is expensive and time consuming. Therefore, the pilot must have as many flight planning aids as possible to help him prepare. The plots provided him should be accurate and realistic flightpath predictions based on sound theory and actual flight test verification.

In order to do this a mathematical model must be derived that includes all pertinent flightpath relationships. Computer simulations can then be run on the model to construct theoretical plots of the flightpath relationships. Once these plots have been made, actual flights should be flown to verify the model.

OBJECTIVE

The objective of this chapter is to derive the mathematical equations to be used in a computer simulation for predicting essential flightpath parameters.

THE MANEUVER

Before a mathematical model can be derived, the type of maneuver that the pilot will perform must be known. There are any number of different maneuvers that can be flown. What is important is that the maneuver is relatively simple and above all repeatable. The maneuver selected for this paper will be referred to as a standard maneuver. It is one that has been attempted in flight tests with some degree of success. The characteristics of the maneuver are:

1. The target drone makes a level turn at the commanded g level. The g profile during the turn approximates a first order lag as depicted in figure 7.
2. The target engine rpm is set at the initiation of the turn and remains fixed throughout the maneuver.
3. The pipper in the launch aircraft is set at a fixed depression. For most missiles this will correspond to the boresight angle of the weapon.
4. At the initiation of the turn, the launch aircraft will be directly in trail with the target and will be at predetermined initial conditions of range, speed and power setting.
5. The launcher pilot will track the drone by holding the pipper on the target throughout the maneuver. The power setting of the launcher will also remain fixed throughout the maneuver. This maneuver can be performed with relative ease allowing the pilot time to concentrate on the operation of the weapon. The level turn was chosen because it is the most difficult situation for the missile. Once the level flight performance envelope is established, it should more than suffice for similar launch parameters in a climb or dive.

As mentioned before, this is only one maneuver and many variations can be made. The equations for the computer model will be similar, however, and the following derivation can be altered to fit any number of different maneuvers.

Attack Situation

Consider this paper as the horizontal plane. The target is making a level turn and the launcher pilot is tracking it with a fixed pipper.

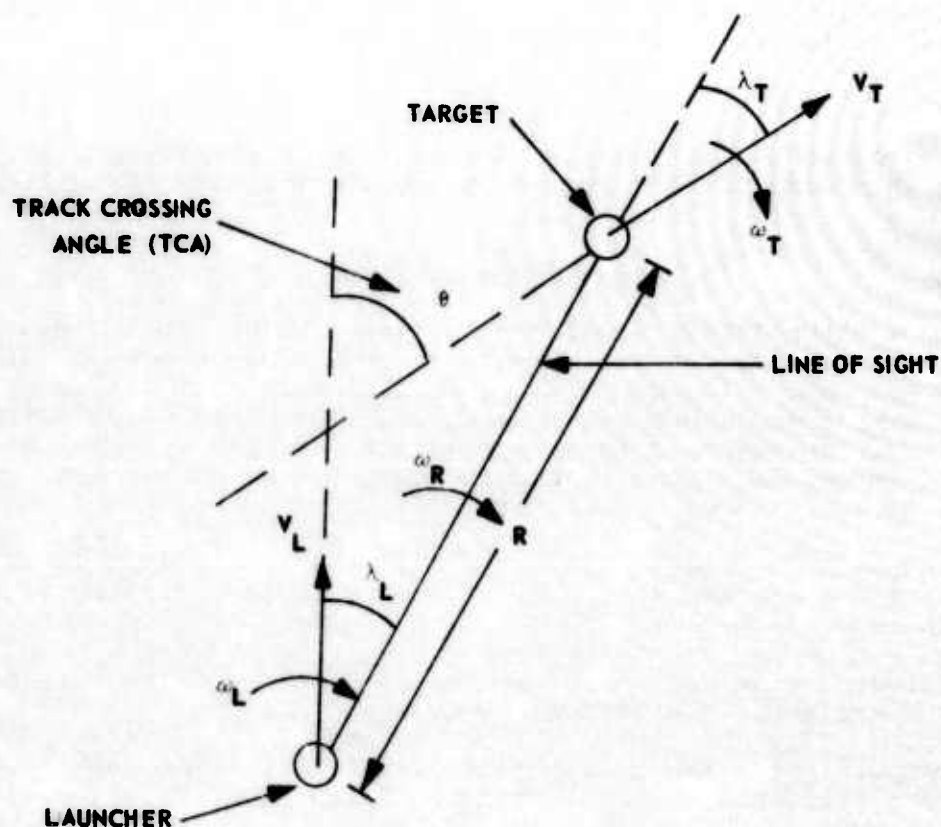


Figure 8 Attack Situation

Where

v_T = target velocity

ω_T = target rate of turn

λ_T = angle between target velocity vector and the line of sight

R = slant range

θ = track crossing angle (i.e., the angle between velocity vectors of launcher and target)

V_L = launcher velocity

ω_L = launcher rate of turn

λ_L = angle between launcher velocity vector and the line of sight

The ultimate aim of this derivation is to find the values of R and θ throughout the maneuver.

From figure 8

$$\theta = \lambda_T + \lambda_L \quad (2.1)$$

Unfortunately, R , λ_T and λ_L are not directly related to ω_T , ω_L , V_T , and V_L . However, their derivatives with respect to time, \dot{R} , $\dot{\lambda}_T$, and $\dot{\lambda}_L$ are directly related. From figure 2, these relationships are

$$\dot{\lambda}_T = \omega_T - \omega_R \quad (2.2)$$

$$\dot{\lambda}_L = \omega_R - \omega_L \quad (2.3)$$

$$\dot{R} = V_T \cos \lambda_T - V_L \cos \lambda_L \quad (2.4)$$

\dot{R} , $\dot{\lambda}_T$, and $\dot{\lambda}_L$ can now be integrated to give R , λ_T , and λ_L for any particular time. θ can be determined from λ_L and λ_T (equation 2.1). The approach, therefore, will be to derive a set of first order differential equations and integrate them to get the required variables. The results can then be plotted to give relative trajectories with respect to time. Integration of the equations can be done either through an analog computer program or by application of some numerical analysis scheme in conjunction with a digital computer program. The latter technique is used for the analysis presented in this paper.

TARGET FLIGHTPATH VARIABLES

To solve for equations 2.2, 2.3, and 2.4, relationships must be found to determine the values of ω_T , ω_R , ω_L , V_T , and V_L at any particular

time. A relationship for ω_R is quite easy to find, and can be derived directly from figure 8; i.e., since ω_R is the angular rate of rotation of the line of sight vector in the horizontal plane, it is a result of the combined effect of target and launcher rotation about each other. In other words, by holding the launcher fixed and determining the rate of rotation of target about it, the resulting equation is

$$\omega_R = \frac{V_T \sin \lambda_T}{R} \quad (2.5)$$

Now by holding the target fixed and allowing the launcher to move, the angular rate is,

$$\omega_R = \frac{V_L \sin \lambda_L}{R} \quad (2.6)$$

The total ω_R is the combined effect, i.e.,

$$\omega_R = \frac{V_T \sin \lambda_T + V_L \sin \lambda_L}{R} \quad (2.7)$$

All that is required now is to develop relationships for ω_T , ω_L , V_T , and V_L . For the sake of continuity the target will be considered first and then the launcher.

Determination of V_T

The velocity of the target can be determined from a first order differential equation derived from Newton's second law

$$F = m a$$

In terms of drone variables, this becomes

$$(T_T - D_T) = \frac{W_T}{g} \frac{d(V_T)}{dt} \quad (2.8)$$

where

T_T = Thrust of the target

D_T = Drag of the target

W_T = Weight of the target

V_T = True velocity of the target

g = Acceleration due to gravity (32.2 ft/sec²)

Rearranging

$$\frac{d(V_T)}{dt} = \dot{V}_T = \frac{(T_T - D_T) g}{W_T} \quad (2.9)$$

The thrust of the target is set at the initiation of the turn, and remains constant throughout the turn. (This may not be true when there are large excursions in velocity.) The value for thrust can be determined from flight test data. The drag increases as the target load factor is increased and can be determined from the target's drag polar.

$$D_T = \left[C_{D0T} + \frac{C_{LT}^2}{\pi AR_T e_T} \right] \frac{1}{2} \rho V_T^2 S_T \quad (2.10)$$

where

C_{D0T} = Zero lift drag of the target

C_{LT} = Lift coefficient of the target

AR_T = Aspect ratio of the target

e_T = Oswald's efficiency factor for the target

ρ = Air density

S_T = Wing area of the target.

C_{D0T} and e_T are constants for speeds less than critical Mach number and can be determined from flight test data. For speeds substantially greater than critical Mach number, separate functions for these parameters should be included. These may also be determined from flight test data. For simplification: C_{D0T} and e_T will be considered to be constants for this analysis.

C_{LT} can be determined directly from the target's load factor, i.e.,

$$n_T = \frac{L_T}{W_T} = \frac{C_{LT} \frac{1}{2} \rho V_T^2 S_T}{W_T} \quad (2.12)$$

Therefore

$$C_{LT} = 2 \frac{n_T W_T}{\rho V_T^2 S_T} \quad (2.12)$$

All that remains to be found is n_T . The target g profile is fixed according to the autopilot's preprogrammed control function. As seen from figure 7 this profile approximates a first order lag. Therefore, the equation for a first order lag can be used, i.e.,

$$n_T = (n_C - 1) (1 - e^{-\frac{t}{\tau}}) + 1 \quad (2.13)$$

where

n_T = target load factor

n_C = commanded steady state g

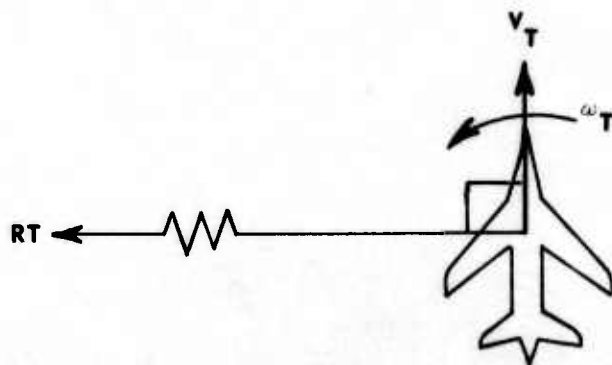
τ = time constant.

It can be seen by inspection that at $t = 0$, $n_T = 1$, and at $t = \infty$, $n_T = n_C$. In between these two extremes, the shape of the function depends upon the value of τ . This value can be easily extracted from drone flight test data.

There are several alternate methods that can be used to determine target velocity. For one, raw test data can be used as an input to the computer simulation. For another, mathematical expressions can be used to approximate the velocity profiles obtained from test data. A third alternative is to solve equation 2.10 according to a known flight test g profile, and then perturb the values of C_{D0T} and e_T until the corresponding velocity profile is identical to flight test values. The resulting values of C_{D0T} and e_T can then be used with equation 2.10 for the computer simulation. Regardless of the method used, V_T can be determined fairly accurately for the computer simulation.

Determination of ω_T

The term, ω_T , is the rate of turn of the target's velocity vector and can be visualized in figure 9.



WHERE:
RT = RADIUS OF TURN

Figure 9 An Aircraft In a Level Turn

Since RT and V_T remain at right angles to each other

$$RT \cdot \omega_T = V_T \quad (2.14)$$

Therefore

$$\omega_T = \frac{V_T}{RT} \quad (2.15)$$

To find the radius of turn (RT) consider an airplane in a turn (figure 10).

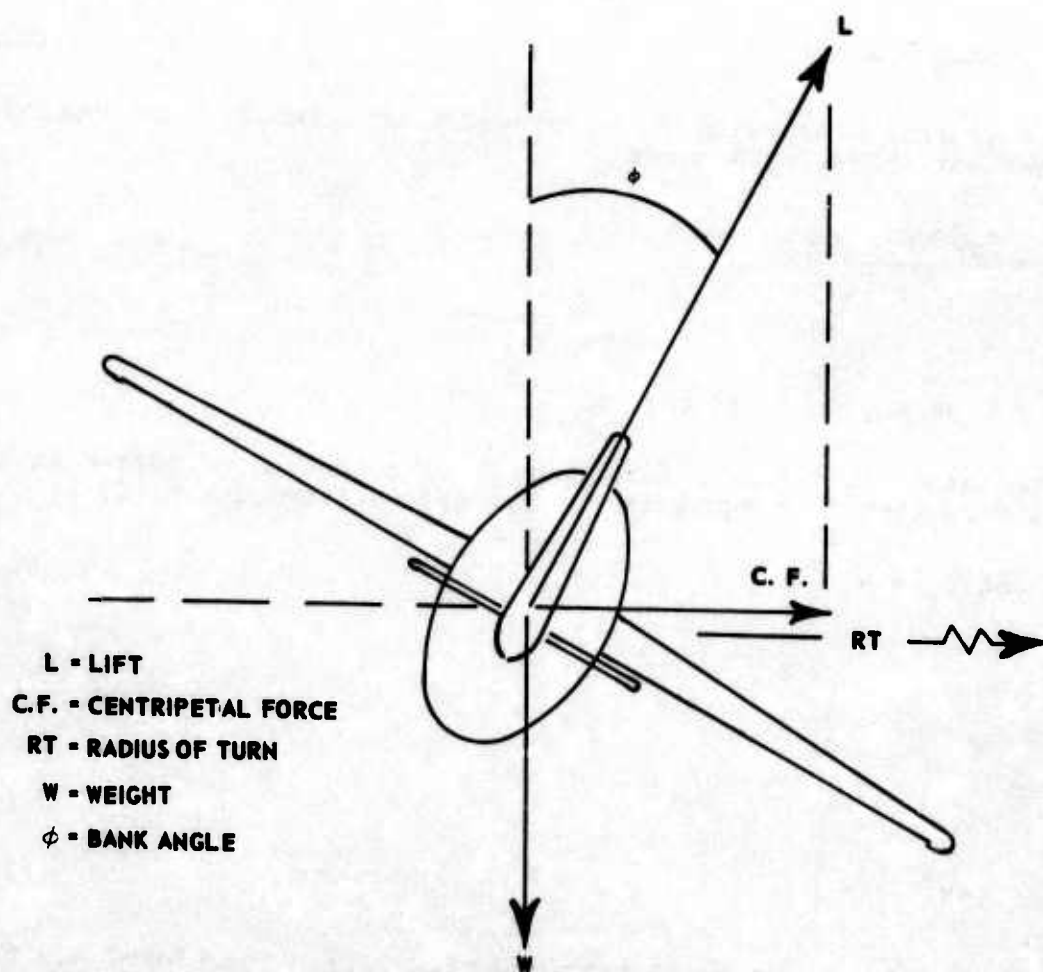


Figure 10 Aircraft in a Bank

The centripetal force (C.F.) relationship is,

$$C.F. = \frac{mV^2}{RT} \quad (2.16)$$

also from figure 10

$$C.F. = L \sin \phi \quad (2.17)$$

Equating the two and solving for RT,

$$RT = \frac{V^2}{ng \sin \phi} \quad (2.18)$$

but since,

$$\omega = \frac{V}{RT} \quad (2.19)$$

then

$$\omega = \frac{ng \sin \phi}{V} \quad (2.20)$$

This is a general expression for an aircraft in a level turn. Substituting the target variables, it becomes

$$\omega_T = \frac{n_T g \sin \phi_T}{V_T} \quad (2.21)$$

where

$$\phi_T = \text{bank angle of the target}$$

Since the target is making a level turn, the summation of forces in the vertical direction must equal zero. Therefore, from figure 10,

$$L_T \cos \phi_T = W_T \quad (2.22)$$

so that

$$\cos \phi_T = \frac{W_T}{L_T} = \frac{1}{n_T} \quad (2.23)$$

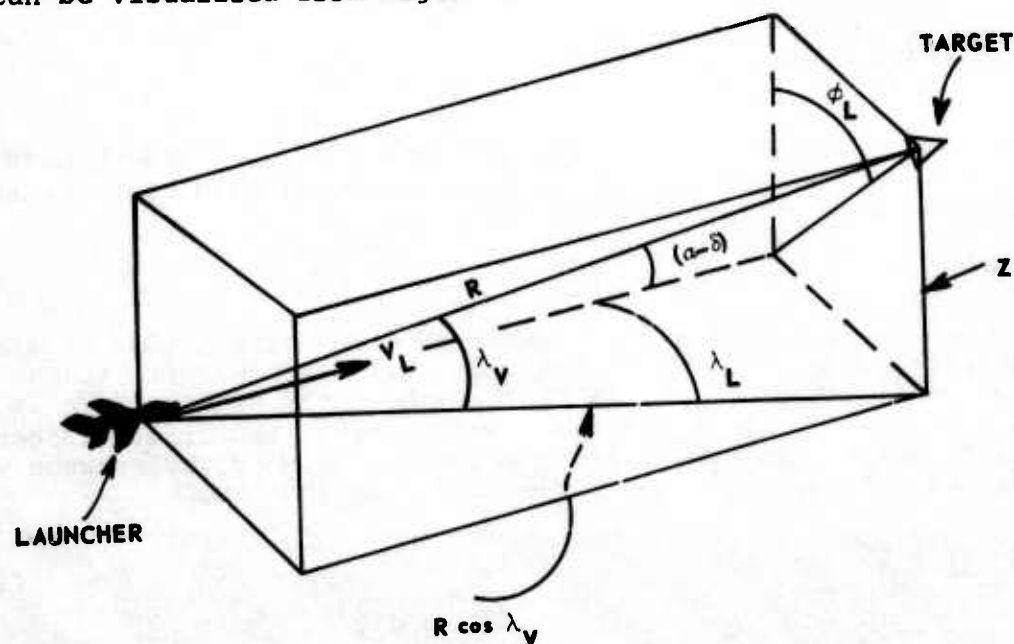
or

$$\phi_T = \cos^{-1} \left(\frac{1}{n_T} \right) \quad (2.24)$$

The term, ω_T , can now be found from equation 2.21. Therefore, equations for all of the pertinent flight variables for the target have been derived. A summary of these equations can be found on pages 29 and 30.

EXPANSION TO THREE DIMENSIONS

It would be nice to continue this derivation in two-dimensional space; however, due to the real-life situation it cannot be done. The pilot is required to hold the pipper on the target using pitch and bank. As a result, he is not attempting to make a level turn, and the launch aircraft may climb or descend during the maneuver. Since the launch aircraft's load factor and velocity are very sensitive to these inputs, the vertical dimension must be taken into account. The three-dimensional picture can be visualized from figure 11.



WHERE:

- α = ANGLE OF ATTACK OF LAUNCHER
- δ = SIGHT DEPRESSION ANGLE
- ϕ_L = LAUNCHER BANK ANGLE
- λ_V = ANGLE BETWEEN LINE OF SIGHT AND THE HORIZONTAL PLANE ADJACENT TO LAUNCHER
- Z = VERTICAL DISTANCE BETWEEN THE TARGET AND THE LAUNCHER

Figure 11 Three-Dimensional View of Attack Situation

Before continuing any further, it is necessary to correct equation 2.7, (determination of ω_R). This equation was originally derived assuming R fell in the horizontal plane. This is not true in the three-dimensional case, therefore $R \cos \lambda_V$ must be substituted for R and the equation becomes

$$\omega_R = \frac{V_T \sin \lambda_T + V_L \sin \lambda_L}{R \cos \lambda_V} \quad (2.25)$$

Now the flight path variables for the launcher can be derived.

LAUNCHER FLIGHTPATH VARIABLES

By substituting the launcher variables into equation 2.20, the equation becomes,

$$\omega_L = \frac{n_L g \sin \phi_L}{V_L} \quad (2.26)$$

Therefore relationships of the three variables, n_L , ϕ_L , and V_L must be derived to solve for ω_L . Once these four variables have been determined, the launchers flight path will be defined.

Determination of V_L

This can be done in the same manner as the determination of the target's velocity (page 18). Since the pilot sets the throttle at the initiation of the turn and leaves it throughout the maneuver, V_L is simply a function of the difference between thrust and drag. (Since the target performance variables are subscripted, launcher performance variables will be left without subscripts to reduce clutter.)

$$\dot{V}_L = \frac{(T - D) g}{W} \quad (2.27)$$

where:

T = Thrust of the Launcher

D = Drag of the Launcher

W = Weight of the Launcher

Thrust can be determined in a variety of ways. Probably the easiest and most accurate would be to leave the thrust at the setting that gives unaccelerated flight at the initial velocity (V_{L0}). In actual flight test, this "trim shot" can be made on the final approach to the launch area. Thrust throughout the maneuver can then be determined by the initial conditions, i.e.,

$$T = D_0 = \left(C_{D0} + \frac{C_L^2}{\pi A R e} \right) \frac{1}{2} \rho V_{L0}^2 S \quad (\text{i.e., at } t = 0) \quad (2.28)$$

Other thrust settings can be used if desired, and can be found from flight manuals or flight test data by obtaining the power setting to hold a particular airspeed. This airspeed can then be used as V_{L0} in equation 2.28 to determine the thrust for the computer simulation. The drag for the launcher can be determined in the same manner as it was for the target, i.e., the launcher drag polar is,

$$D = \left(C_{D0} + \frac{C_L^2}{\pi AR e} \right) \frac{1}{2} \rho V_L^2 S \quad (2.29)$$

where:

C_{D0} = Zero lift drag coefficient of the launcher

C_L = Coefficient of lift of the launcher

AR = Aspect ratio of the launcher

e = Oswald's efficiency factor for the launcher

V_L = Launcher true velocity

S = Wing area of the launcher.

Once again C_{D0} and e can be determined from flight test data. C_L is determined by the pilot inputs to the longitudinal control. As the pilot pulls the stick back to hold the pipper on the target, he increases the launcher angle of attack (α), which in turn increases C_L according to the equation

$$C_L = \frac{\partial C_L}{\partial \alpha} \cdot \alpha \quad (2.29)$$

(Assumes a linear C_L vs α curve for the launcher)

Note: $\frac{\partial C_L}{\partial \alpha}$ can be determined from flight test data.

The term, α , is determined by the geometric relationship between the launcher and the target. Since it is the direct result of the pilot's input, it can best be analyzed in conjunction with ϕ_L (launcher bank angle).

Determination of ϕ_L and α

These are the pilot inputs. The pilot banks the aircraft (ϕ_L) and pulls or pushes on the stick (α) to hold the pipper on the target; and since he is top gun in his squadron he always holds the pipper exactly on the target. As a result of this constraint, the launch aircraft does not fly a level turn, but must climb or descend to make the angular relation hold. This geometric relationship between the launcher and the target can be seen in figure 11.

The depression angle, δ , can be any predetermined value, but usually will be the angle that aligns the pipper with the sensor head of the missile in the caged position. For instance, when the AIM-9E is on an F-4, the missile head is aimed 2 degrees below the fuselage reference line in the caged position. Therefore, if the pilot depresses his sight 2 degrees and puts the pipper on the target, he will be pointing the sensor directly at the target. Since this allows for easy operation of the missile, it is the most desirable setting for the mission.

From figure 11, we see

$$R \sin (\alpha - \delta) \sin \phi_L = R \cos \lambda_V \sin \lambda_L \quad (2.30)$$

cancelling the R's

$$\sin (\alpha - \delta) \sin \phi_L = \cos \lambda_V \sin \lambda_L \quad (2.31)$$

Also from figure 11,

$$R \sin (\alpha - \delta) \cos \phi_L = R \sin \lambda_V \quad (2.32)$$

or

$$\sin (\alpha - \delta) \cos \phi_L = \sin \lambda_V \quad (2.33)$$

By dividing equation 2.31 by equation 2.33, we get

$$\tan \phi_L = \cot \lambda_V \sin \lambda_L \quad (2.34)$$

so that

$$\phi_L = \tan^{-1} (\cot \lambda_V \sin \lambda_L) \quad (2.35)$$

Also from equation 2.31

$$\sin (\alpha - \delta) = \frac{\cos \lambda_V \sin \lambda_L}{\sin \phi_L} \quad (2.36)$$

Therefore

$$\alpha = \sin^{-1} \left(\frac{\cos \lambda_V \sin \lambda_L}{\sin \phi_L} \right) + \delta \quad (2.37)$$

Determination of n_L

Once α is known, C_L can be found from equation 2.29, and then n_L from the equation,

$$n_L = \frac{L}{W} = \frac{C_L \rho V_L^2 S}{2W} \quad (2.38)$$

Therefore, ϕ_L and n_L can be found if λ_V and λ_L are known at any particular time. Remember λ_L is determined by integrating $\dot{\lambda}_L$ (equation 2.3). The term, λ_V , must also be determined by integrating $\dot{\lambda}_V$ since λ_V is a function of the vertical velocity of the launch aircraft. From figure 11,

$$\sin \lambda_V = \frac{Z}{R} \quad (2.39)$$

differentiating,

$$\frac{d(\sin \lambda_V)}{dt} = \frac{d\left(\frac{z}{R}\right)}{dt} \quad (2.40)$$

which is,

$$\cos \lambda_V \frac{d(\lambda_V)}{dt} = \frac{1}{R} \frac{dz}{dt} - \frac{z}{R^2} \frac{dR}{dt} \quad (2.41)$$

or

$$\frac{d(\lambda_V)}{dt} = \dot{\lambda}_V = \frac{1}{R \cos \lambda_V} (\dot{z} - \frac{z}{R} \dot{R}) \quad (2.42)$$

substituting,

$$\dot{z} = V_{V_L} \text{ (vertical velocity of launcher)} \quad (2.43)$$

and

$$z = R \sin \lambda_V \quad (2.44)$$

we get

$$\dot{\lambda}_V = \frac{1}{R \cos \lambda_V} (V_{V_L} - \sin \lambda_V \dot{R}) \quad (2.45)$$

Now all that is required is to find V_{V_L} . The launcher's vertical velocity is dependent upon the pilot inputs. The aircraft is controlled by the constraint that the pipper must be held on the target. The ensuing vertical velocity will result from an unequal force in the vertical direction (ΔF_V).

$$\Delta F_V = m \dot{V}_{V_L} = \frac{W}{g} \dot{V}_{V_L} \quad (2.46)$$

and from figure 10,

$$\Delta F_V = W - L \cos \phi_L \quad (2.47)$$

Combining equation 2.46 and 2.47

$$W - L \cos \phi_L = \frac{W}{g} \dot{V}_{V_L} \quad (2.48)$$

multiplying through by $\frac{g}{W}$ and substituting n_L for $\frac{L}{W}$,

$$\dot{V}_{V_L} = g (1 - n_L \cos \phi_L) \quad (2.49)$$

This completes the derivation of the equations to compute the relative trajectories of the two vehicles and the related flightpath parameters.

SUMMARY

A set of first order differential equations now exist that can be used to determine the "state" of the system at any particular time (i.e., λ_L , λ_T , λ_V , V_T , V_L , and R). From this the values for θ and R are determined throughout the maneuver. Plots can now be made showing the relationship of θ and R as time progresses throughout the maneuver. By overlaying these plots on the missile's performance envelope, the proper initial conditions can be determined for arriving at the desired set of launch parameters (figure 12).

LAUNCHER (F-4E)	TARGET (BQM-34A/AIMS)
Weight - 38,000 lbs	Weight - 1,900 lbs
Altitude - 10,000 ft	Altitude - 10,000 ft
Initial Velocity - 850 ft/sec	Initial Velocity - 850 ft/sec
Trim Thrust Velocity - 925 ft/sec	Trim Thrust Velocity - 850 ft/sec

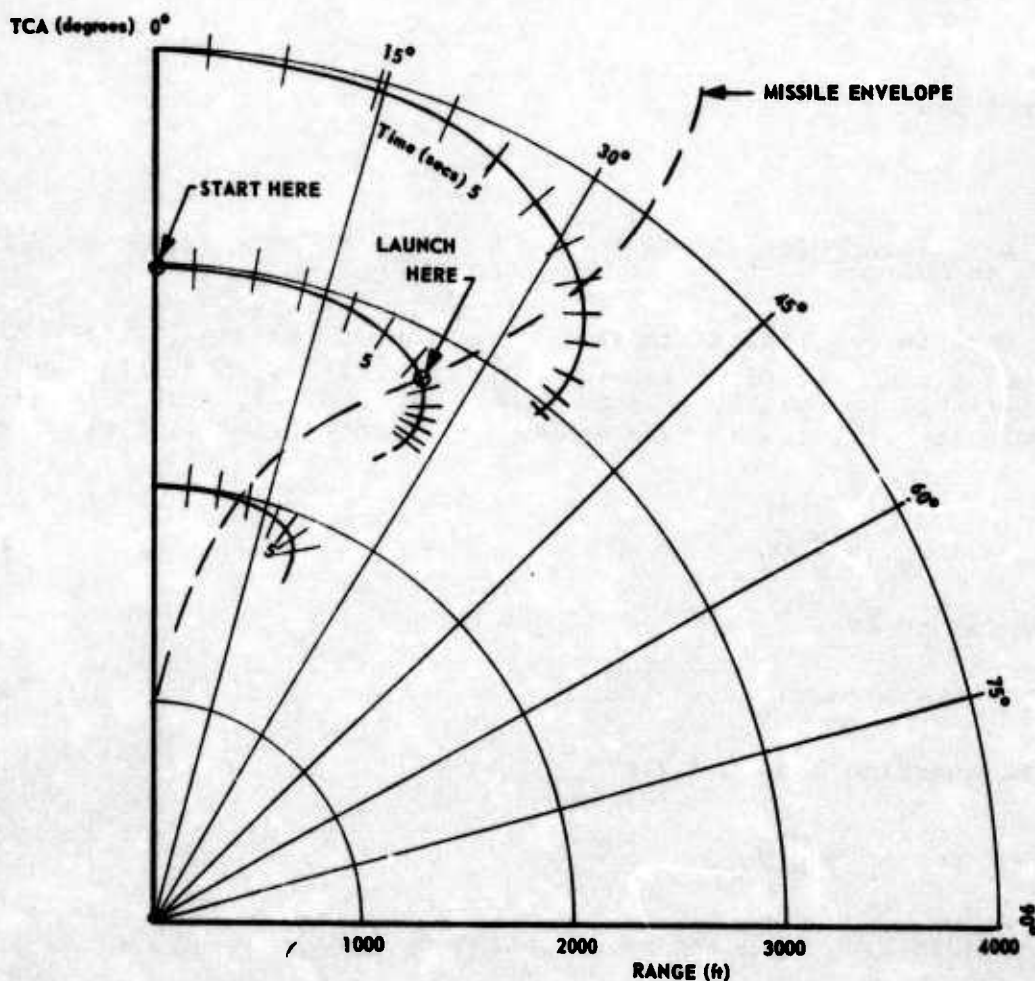


Figure 12 Flight Path Prediction Curves

A summary of the equations derived in this chapter is listed below. The computer program used to compute the trajectories in figure 12 is listed in appendix I.

For convenience a summary of the equations derived in Chapter II are listed below.

STATE EQUATIONS

1. $\dot{\lambda}_T = \omega_T - \omega_R$
2. $\dot{\lambda}_L = \omega_R - \omega_L$
3. $\dot{R} = V_T \cos \lambda_T - V_L \cos \lambda_L$
4. $\dot{V}_L = \frac{(T-D)W}{g}$
5. $\dot{\lambda}_V = \frac{1}{R \cos \lambda_V} (V_{V_L} - \sin \lambda_V \dot{R})$
6. $\dot{V}_{V_L} = g (1 - n_L \cos \phi_L)$
7. $\dot{V}_T = \frac{(T_T - D_T)}{W} g$

CONTROL AND RELATED EQUATIONS

1. $n_T = (n_c - 1) (1 - e^{-\frac{t}{\tau}}) + 1$
2. $\phi_T = \cos^{-1} \left(\frac{1}{n_T} \right)$
3. $T = \left(C_{D0} + \frac{C_{L0}^2}{\pi AR e} \right) \frac{1}{2} \rho V_{L0}^2 S$
4. $C_{L0} = \frac{2 W}{\rho V_{L0}^2 S}$
5. $D = \left(C_{D0} + \frac{C_L^2}{\pi AR e} \right) \frac{1}{2} \rho V_L^2 S$
6. $C_L = \frac{2 n W}{\rho V_L^2 S}$
7. $\phi_L = \tan^{-1} (\cot \lambda_V \sin \lambda_L)^*$

*If $\lambda_V = 0$, then ϕ_L goes to infinity. This should be considered carefully in any computer program.

8. $\alpha = \sin^{-1} \left(\frac{\cos \lambda_V \sin \lambda_L}{\sin \phi_L} \right) + \delta$
9. $n_L = \frac{C_{L\alpha} \rho V_L^2 S}{2 W}$
10. $\theta = \lambda_T + \lambda_L$
11. $\omega_T = \frac{n_T g \sin \phi_T}{V_T}$
12. $\omega_L = \frac{n_L g \sin \phi_L}{V_L}$
13. $\omega_R = \frac{V_T \sin \lambda_T + V_L \sin \lambda_L}{R \cos \lambda_V}$
14. $D_T = \left(C_{D0T} + \frac{C_{LT}^2}{\pi A R_T e_T} \right) \frac{1}{2} \rho V_T^2 S_T$
15. $T_T = D_T(t = 0)$

CHAPTER III

TEST TECHNIQUES

BACKGROUND

A great deal of time and effort has been spent in this area by many different agencies. A variety of methods have been developed and a myriad of equipment has been used to help the pilot launch a missile at the proper set of parameters. Some techniques have been relatively successful, however quite often they are so complicated that they cause more problems than they solve. A good example of this was one in which the pilot was so burdened with aids, procedures, and complicated techniques that he neglected to lock the missile onto the target prior to launching it. The technique presented here should never be construed to be the only way to solve the problem. It does have certain advantages in that it is relatively simple, inexpensive and requires a minimum of pilot workload. It is somewhat unique in that it requires a departure from traditional procedures of test planning. The most important facet, however, is that within the limits of the equipment, it will guarantee that the missile is launched at the edge of its predicted envelope.

OBJECTIVE

The objective of this chapter is to present a simple and inexpensive way to insure that the missile is fired at the edge of its envelope. The method presented is composed of three basic elements.

1. Establishment of a set of acceptable launch conditions in the vicinity of the desired launch conditions. (Remember a launch condition is one set of the parameters range, TCA and target g.)
2. Real time computation of flightpath relationship during the test.
3. A "fire signal".

In a nutshell, the test method is to have a matrix of acceptable launch conditions, measure the parameters as the pilot is making the attack, and generate a "fire signal" when an acceptable launch condition is reached.

ACCEPTABLE LAUNCH CONDITIONS

As mentioned before this method represents a departure from traditional test planning procedures. Previously, the pilot has been given one set of launch parameters. He was to do whatever he could to get to that set of parameters and then launch the missile. Any miscalculation on his part or the part of the drone controller resulted in an error. Since flightpath parameters change so quickly during this type of maneuver, relatively small miscalculations can result in substantial errors. Therefore, regardless of how sophisticated the test method is, this approach is highly susceptible to errors.

One solution to this problem is to remove the constraint of having only one launch condition. By making a list of acceptable conditions all based on the "edge of the envelope" criteria, and by allowing the pilot to fire when he reaches anyone of these conditions, the pilot's problem is extremely simplified. Under this concept there is no need to provide sophisticated aids to guide the pilot to the proper launch point. All that is required is a system to tell the pilot when he has reached an acceptable condition.

This does not eliminate the need for a desired launch point. The pilot will still plan and fly his attack as if he were after one set of parameters. In case of a miscalculation, however, alternate launch points will be provided. The criteria for these alternate points are:

1. They fall on the edge of predicted missile performance envelope.
2. They are acceptable to all agencies involved (i.e., they are not repeats of points already tested, etc.).

The acceptability criteria is the unique aspect of this method. Although this paper does not concern itself with test management, it should be pointed out that certain ground rules must be agreed upon early in the test planning phase to forego any contractual problems. The success of this technique depends upon the use of alternate launch points. If these were eliminated for other than technical reasons, it would seriously limit the probability of success.

SELECTING ALTERNATE LAUNCH POINTS

This can best be shown by example. Consider the hypothetical case in which a set of missile performance envelopes for a particular altitude, target Mach number and launcher overtake have been provided. Target g varies from 2 g's to 5 g's in 0.2-g increments. A desired set of launch parameters have been provided and are:

1. Target load factor - 4 g's
2. Range - 3,500 feet
3. TCA - 30 degrees

Also the limits to the acceptable launch conditions are:

1. Target g - 3.6 to 4.4 g's
2. Range - 3,000 to 4,000 feet
3. TCA - 25 to 35 degrees

Using this information a matrix of alternate launch conditions can be constructed. This can be done in the following manner (figure 13).

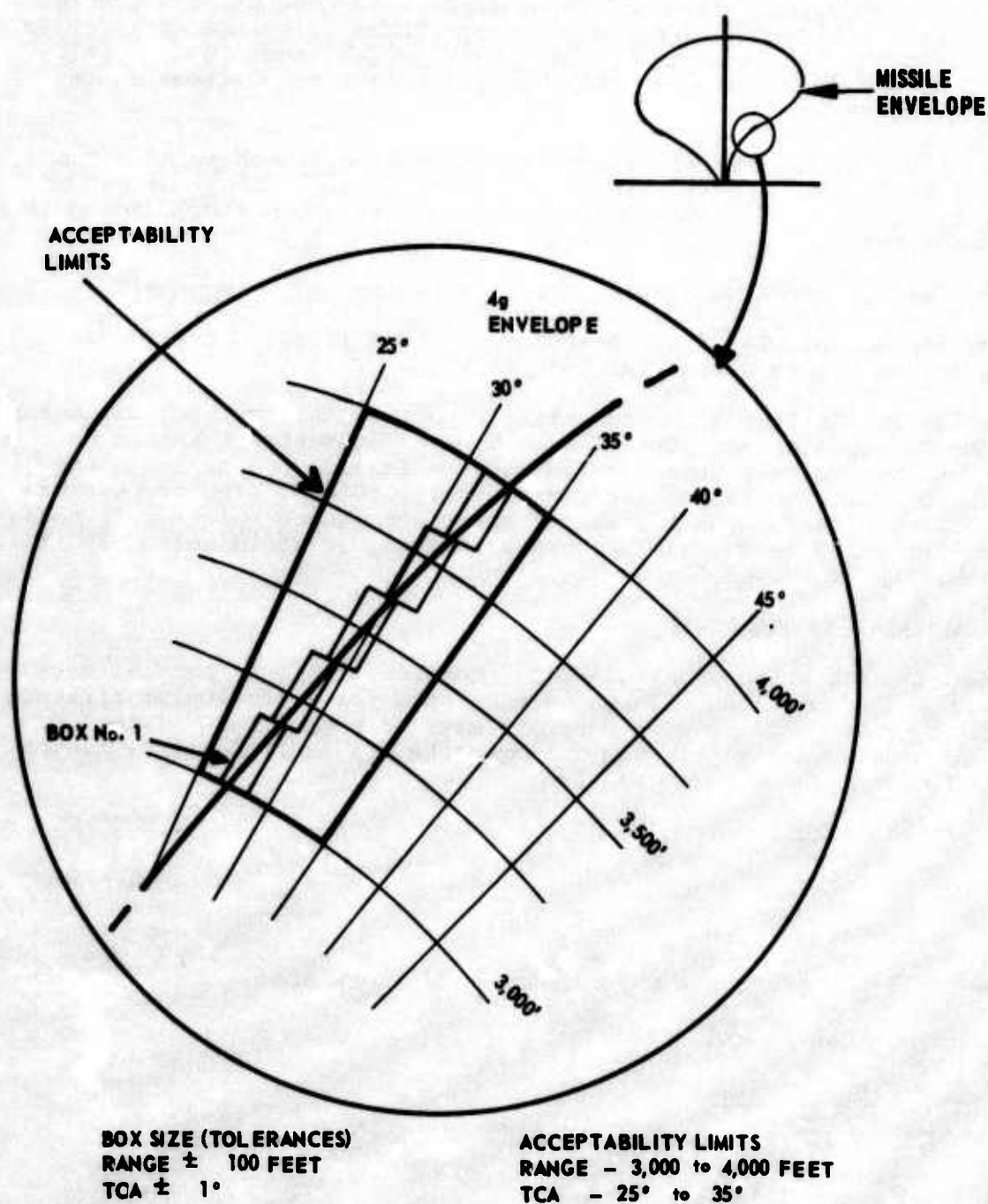


Figure 13 Construction of Acceptable Launch Parameter Matrix

1. On the 4-g envelope, draw lines that represent the limiting values of range and TAC (acceptability limits).
2. Establish launch point tolerances. These tolerances establish the size of the "boxes" to be used in constructing the matrix. They could be based on the accuracy of the equipment, or they may be picked to satisfy any number of other test requirements. For this example they will be arbitrarily picked at
 - a. Target load factor ± 0.1 g
 - b. Range ± 100 feet
 - c. TCA ± 1 degree
3. Along the edge of the 4-g envelope plot a series of adjacent boxes in which each box covers an area based on the tolerances listed above.
4. Perform steps 1 and 3 for each envelope available from 3.6 g's to 4.4 g's (acceptability limits for g's).
5. On each of these plots, measure the values of range and TCA at the extremities of each box.
6. Using these values create a matrix of alternate launch conditions (figure 14).

Target Load Factor (g's)	3.5 - 3.7	3.7 - 3.9	3.9 - 4.1*	4.1 - 4.3	4.3 - 4.5
BOX No. 1			3000'	26°	
			3200'	28°	
BOX No. 2			3200'	27.5°	
			3400'	29.5°	
BOX No. 3			3400'	28.5°	
			3600'	30.5°	
BOX No. 4			3600'	30°	
			3800'	32°	
BOX No. 5			3800'	31°	
			4000'	33°	

* These Data Were Taken From The 4.0 g Envelope.

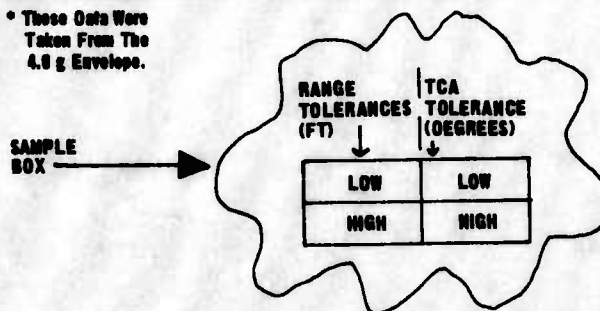


Figure 14 Matrix of Acceptable Launch Conditions

After running through this example, there are two problems that come to mind. First of all, there is a possibility that the missile can be launched inside one of the boxes but just outside the edge of the envelope. This results from plotting the center of the box on the envelope's edge. A more conservative approach would be to plot the outside extremity of the box on the edge of the envelope. The center of the box would then fall just inside of the edge. Although this is a compromise, it may be necessary to preclude the possibility of having to invalidate the test.

Secondly, if envelopes are not provided at increments of target g that are commensurate with the g tolerance, there will be gaps in the matrix. In this case it may be necessary to interpolate between the envelopes provided, or request additional plots.

Once these problems are solved, and a matrix of acceptable conditions is approved, the method can be easily implemented. The matrix is stored in a computer and compared with real time flight parameters. All that is left is to set up equipment to measure real time flightpath parameters and generate a "fire signal".

REAL TIME FLIGHTPATH COMPUTATION

This can be done any number of ways. The objective is to obtain values for range, TCA, and target g as the attack is being performed. Probably the simplest and most inexpensive way to do this is to use FPS-16 radar to measure range and TCA, and existing drone telemetry to obtain target g . Since this equipment is standard for most missile tests, there is no requirement for additional instrumentation. The information can easily be tapped and sent to a central computer (figure 15). The computer processes the information, compares it with the stored matrix of acceptable conditions, and when it finds a match, sends a "fire signal" to the pilot.

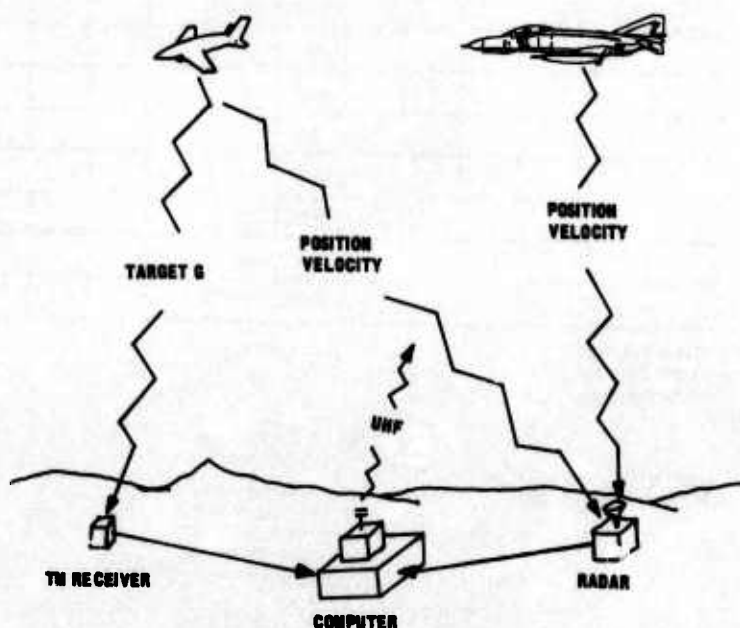


Figure 15 Real Time Computation of Flight Path Parameters

THE "FIRE" SIGNAL

To properly analyze radar and telemetry information so that the fire signal will have the proper effect, all delays must be accounted for. In all cases, there will be a delay between the time the parameters are measured and the missile is launched. Such things as computer computation time, pilot's response time and missile delays during the launch sequence can add up and must be considered.

To compensate for these delays a method of predicting launch conditions must be used. In other words, the computer must use "predicted" parameters rather than existing parameters to compare with the stored matrix of acceptable conditions. Therefore, rate of change of range and TCA must be computed. This can be done by taking derivatives of the measured values, however, special care must be taken to properly smooth or filter the information. Once these values are computed, the predicted parameters can be found. For example, predicted range would be,

$$R_p = R_m + \dot{R} \times \Delta t$$

where

R_p = Predicted range

R_m = Measured range

\dot{R} = Computed rate of change of R_m

Δt = Time delay.

Predicted range and predicted TCA (θ_p) are then compared with the acceptable conditions. There is no need to compute a predicted target g since by necessity it is a constant.

The "fire signal" is generated when the values of target g , R_p and θ_p are the same as one of the stored acceptable conditions. A typical flow diagram for this type of program can be seen in figure 16. The signal can be generated in a variety of ways, however, an aural tone over the UHF radio appears to be preferable, since it is simple and inexpensive. What ever it is, certain criteria should be met.

1. It must be unique so that no other signals could be mistakenly interpreted as a fire signal.
2. It should not distract the pilot from his primary task, which is tracking the target, locking the missile onto the target, and launching the missile.
3. It should not mask other important signals, such as an aural tone from the missile, etc.
4. If it is aural, it should be terminated at launch. Good communications after launch are essential to flight safety.

COMPUTER LOGIC

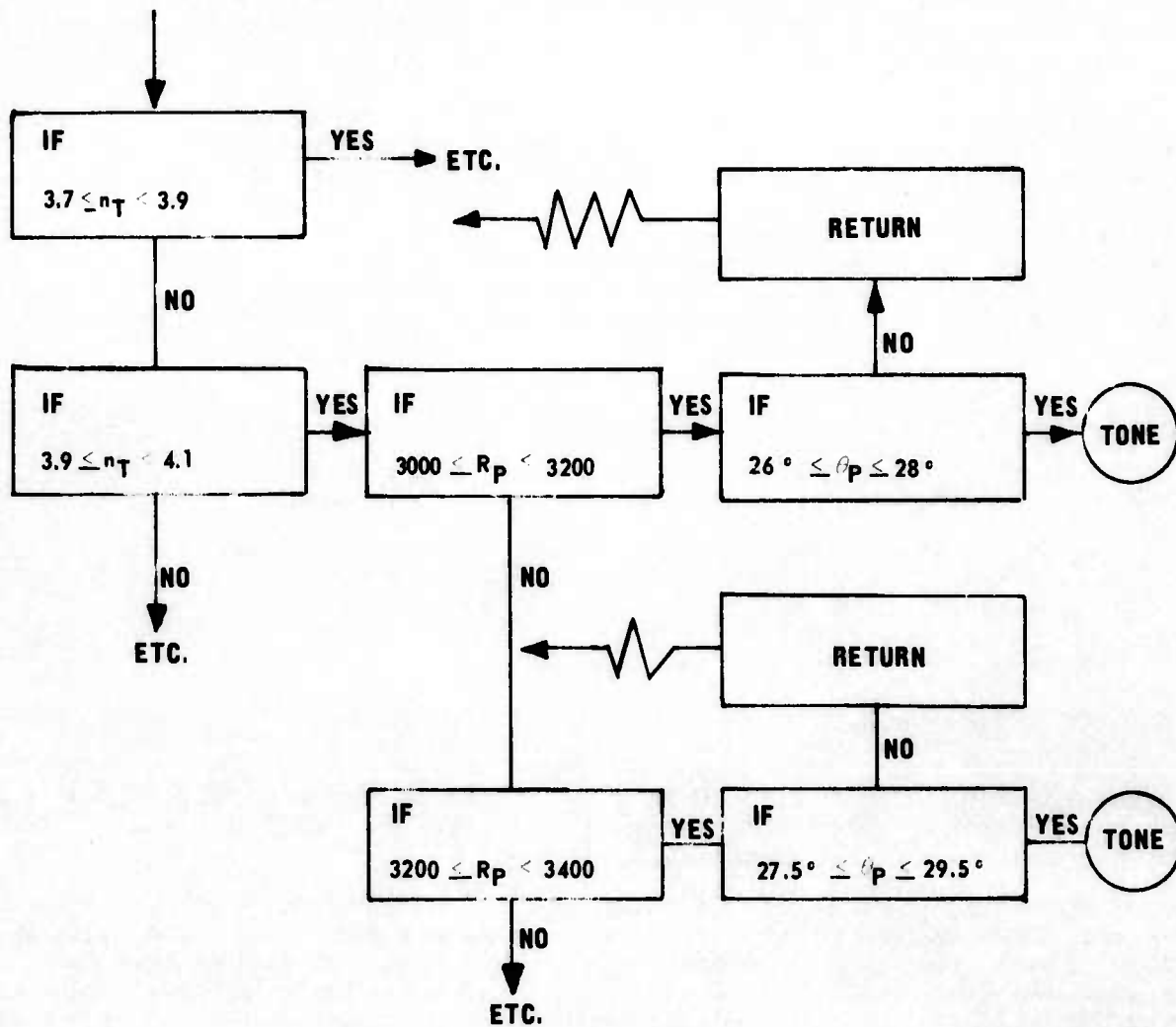


Figure 16 Flow Diagram For Comparison of Predicted Parameters with Acceptable Conditions

LAUNCHER AND TARGET VELOCITIES

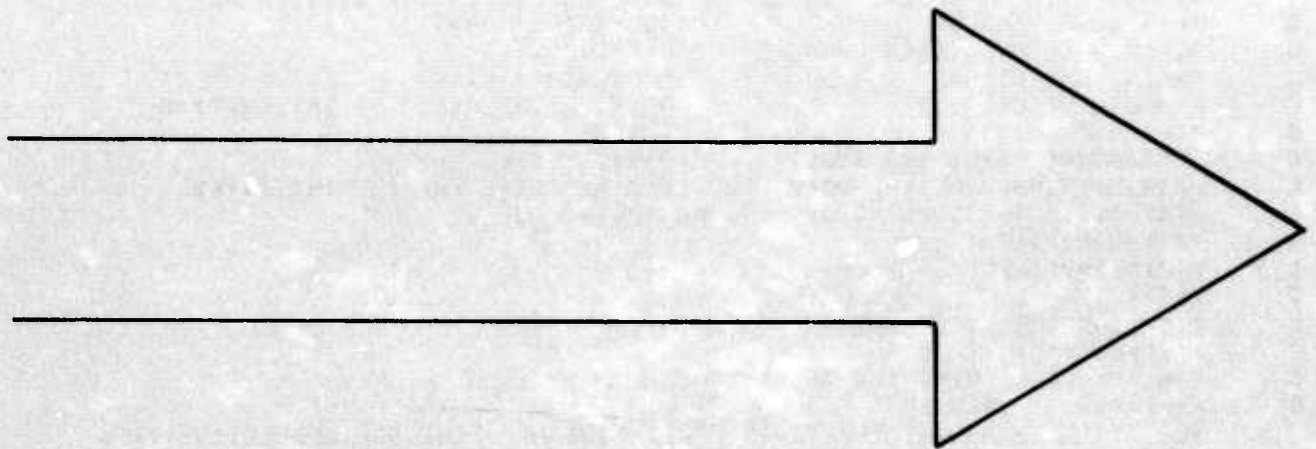
No mention has been made of controlling the velocity of the target or the launcher. This, of course, could be done by requiring the pilot and drone controller to monitor airspeeds and adjust the throttle accordingly. However, this additional task increases the complexity of the maneuver and the possibility of human error. In addition, experience has shown that the proper velocities can best be obtained by establishing the proper initial conditions, holding the thrust fixed, and allowing the airspeed to vary according to a predetermined schedule. Fortunately the missile performance envelope is much less sensitive to velocity errors than to errors in the other parameters. Therefore, if the standard maneuver is properly planned and executed, the resulting velocity errors should be small enough to be considered negligible.

SUMMARY

Short range missile testing is a very demanding discipline. The difference between success and failure may often depend on some trivial item that can easily be overlooked. The key to success is preparation. The information presented has been concerned with several of the more important elements of this peculiar type of testing. The techniques and methods are by no means the only way to do it. Careful examination of these methods, however, and any others that have been tried or theorized can be an invaluable aid in planning a short range missile test.

THIS PAGE LEFT BLANK FOR PRESENTATION PURPOSES

APPENDIX I
COMPUTER PROGRAM
AND SAMPLE COMPUTER OUTPUT



#####

COMPUTER PROGRAM

SRMT TRACE

CDC 6400 FTN V3.0-P336 OPT=1 04/13/73

PROGRAM SRMT (INPUT, OUTPUT)

DIMENSION Y(7), DY(7), SD(7), Q(7), A(4), B(4), C(4)

REAL NT, NL, NC, LAV, M, LAVP, LAML, LAMT, MT

CALL MAJOR MCATEE, EXT 72348

```

C *****
C W=WEIGHT OF LAUNCHER S=HING AREA OF LAUNCHER
C CLA=SLOPE OF LIFT CURVE-LAUNCHER CDZ=ZERO LIFT DRAG COEF-LAUNCHER
C AR=ASPECT RATIO-LAUNCHER EP=OSWALD EFFICIENCY FACTOR-LAU AND TARG
C TAU=TIME CONSTANT FOR G PROFILE RO=AIR DENSITY
C VL=LAUNCHER VELOCITY VT=TARGET VELOCITY
C RZ=INITIAL RANGE DEL=SIGHT DEPRESSION ANGLE
C NC=COMMANDED G FOR TARGET CLAT=SLOPE OF LIFT CURVE FOR TARGET
C WD=WEIGHT OF DRONE CDZO=ZERO LIFT DRAG COEF-TARGET
C VZ=TRIM VELOCITY FOR DETERMINING THRUST FOR LAUNCHER
C VZT=TRIM VELOCITY FOR DETERMINING THRUST FOR TARGET
C NT=TARGET LOAD FACTOR NL=LAUNCHER LOAD FACTOR
C PHIL=LAUNCHER BANK ANGLE PHIT=TARGET BANK ANGLE
C OMT=OMEGA-T OML=OMEGA-L
C CL=COEFFICIENT OF LIFT-LAUNCHER CLT=COEFFICIENT OF LIFT-TARGET
C THT=TARGET THRUST DOT=TARGET DRAG
C ALFA=ANGLE OF ATTACK-LAUNCHER LAV=LAMDA-V
C TH=LAUNCHER THRUST M=LAUNCHER MASS
C G=ACCEL OF GRAVITY DT=TIME INTERVAL FOR INTEGRATION
C MT=TARGET MASS T=TIME
C THETA=TRACK CROSSING ANGLE OMR=OMEGA-R
C OMRP, OMT, OMLP, PHITP, PHILP, LAUP, LAMT AND LAML ARE THE INDICATED
C VARIABLES CONVERTED TO DEGREES FOR PRINT OUT
C Y(1)=LAMDDA-T
C Y(2)=LAMBDA-L
C Y(3)=RANGE
C Y(4)=LAUNCHER VELOCITY
C Y(5)=LAMBDA-V
C Y(6)=VERTICLE VELOCITY OF LAUNCHER
C Y(7)=TARGET VELOCITY
C ALL DY(I) TERMS ARE THE FIRST DERIVATIVE WRT TIME FOR RESPECTIVE Y(I)
C SD(I), Q(I), A(ND), B(ND), AND C(ND) ARE TERMS FOR PERFORMING INTEGRATION
C *****

```

G=32.2

DT=.1

A(1)=.5

C(1)=.5

A(2)=.292893219

B(2)=A(2)

C(2)=A(2)

A(3)=1.70710678

B(3)=A(3)

C(3)=A(3)

A(4)=.16666667

B(4)=1.0

B(4)=.3333333

C(4)=0

1 READ 10, W, S, CLA, CDZ, AR, EP, TAU, VZ, VZT

15 READ 10, RO, VL, VT, RZ, DEL, NC, CLAT, WD, CDZO

IF (W.EQ.0.00) GO TO 520

10 FORMAT(10F8.0)

SRMT TRACE

CDC 6400 FTN V3.0-P336 OPT=1 04/13/73

```

PRINT 12
12 FORMAT(1H1//////////*) .....THE INPUT VARIABLES A
1RE.....*)
PRINT 16,W,S,CLA,CDZ,AR,EP,TAU,RO,VL,VT,RZ,DEL,NC,CLAT,WD,CDZO,VZ,
1VZT
16 FORMAT( //2X,*W=*,F8.0 / 2X,*S=*,F8.2 / 2X,*CLA=*,F8.4 /
X - 2X,*CDZ=*,
1F8.4 / 2X,*AR=*,F8.4 / 2X,*EP=*,F8.4 / 2X,*TAU=*,F8.4 / 2X,*RO=*,
2F8.5 / 2X,*VL=*,F8.2 / 2X,*VT=*,F8.2 / 2X,*RZ=*,F8.1 / 2X,*DEL=*,
3F8.4 / 2X,*NC=*,F8.4 / 2X,*CLAT=*,F8.4 / 2X,*WD=*,F8.0 / 2X,*CDZO=
4*,F8.4,/,2X,*VZ=*,F8.2,/,2X,*VZT=*,F8.2,////)
PRINT 17
17 FORMAT(1H1//*) TIME PHIT IAR-G T-VEL LAM-T LAM-L T
1META LAU-G PHIL OMEG-L L-VEL RANGE OMEG-R LAM
2-V*)
C *****INITIAL CONDITIONS*****
K=0
KD=0
NT=1
NL=1
Y(1)=0
Y(2)=0
Y(3)=RZ
Y(4)=VL
PHIL=.175
PHIT=0
OMT=0
DO 20 I=1,7
20 DY(I)=0
QST=17.9*RO*VT**2
CLT=WD/QST
THT=(CDZO+CLT**2/13.09)*17.9*RO*VZT**2
DDT=(CDZO+CLT**2/13.09)*QST
QS=.5*RO*VL**2*S
ALFA=W/(CLA*QS)
LAV=ALFA-DEL
Y(5)=LAV
Y(6)=0
Y(7)=VT
CL=W/QS
TH=(CDZ+CL**2/(3.14*AR*EP))*5*RO*VZ**2*S
M=W/G
MT=WD/G
T=0
Y(2)=LAV*TAN(PHIL)
THETA=Y(2)
ALFA=ALFA/COS(PHIL)
NL=CLA*ALFA*QS/W
OML=NL*G*SIN(PHIL)/Y(4)
CL=CLA*ALFA
D=(CDZ+CL**2/(3.14*AR*EP))*QS
95 DO 100 I=1,7
100 Q(I)=0
OMR=(Y(7)*SIN(Y(1))+Y(4)*SIN(Y(2)))/(Y(3)*COS(Y(5)))
OMTP=57.3*OMT

```

SRMT

TRACE

CDG 6400 FIN V3.0-P336 OPT=1 04/13/73

```

OMLP=57.3*OML
OMRP=57.3*OMR
PHITP=57.3*PHIT
PHILP=57.3*PHIL
LAVP=57.3*Y(5)
LAMT=57.3*Y(1)
LAML=57.3*Y(2)
PRINT 510,T,PHITP,NT,Y(7),LAMT,LAML,THETA,NL,PHILP,OMLP,Y(4),Y(3),
1OMRP,LAVP

```

C *****RUNGE KUTTA NUMERICAL INTEGRATION SCHEME*****

```

200 ND=0
201 DY(1)=OMT-OMR
    DY(2)=OMR-OML
    DY(3)=Y(7)*COS(Y(1))-Y(4)*COS(Y(2))
    DY(4)=(TH-D)/M
    DY(5)=(Y(6)-SIN(Y(5))*DY(3))/(Y(3)*COS(Y(5)))
    DY(6)=G*(1.-NL*COS(PHIL))
    DY(7)=(THT-DDT)/MT
    ND=ND+1
    DO 300 I=1,7
        SD(I)=DT*DY(I)
        Y(I)=Y(I)+A(ND)*SD(I)-B(ND)*Q(I)
300 Q(I)=(1.-3.*B(ND))*Q(I)+2.*C(ND)*SD(I)
    GO TO (400,201,400,500),ND
400 T=T+DT/2.
    GO TO 201
500 CONTINUE

```

C*****

C *****TEST FOR SINGULARITY*****

```

IF((Y(5)-.0001).GT.0.0000)GOTO 505
Y(5)=0.0001

```

C *****CONTROL AND RELATED EQUATIONS*****

```

505 PHIL=ATAN(SIN(Y(2))/TAN(Y(5)))
50 QS=.5*RO*Y(4)**2*S
    CL=NL*W/QS
    D=(CDZ+CL**2/(3.14*AR*EP))*QS
    NT=(NC-1.)*(1.-1./EXP(T/TAU))+1.
    PHIT=ACOS(1./NT)
    OMT=NT*G*SIN(PHIT)/Y(7)
    OMR=(Y(7)*SIN(Y(1))+Y(4)*SIN(Y(2)))/(Y(3)*COS(Y(5)))
    QST=.5*RO*Y(7)**2*35.9
    CLT=NT*W/QST
    DDT=(CDZD+CLT**2/13.09)*QST
    ALFA=ASIN(COS(Y(5))*SIN(Y(2))/SIN(PHIL))+DEL
    NL=CL4*ALFA*QS/W
    OML=NL*G*SIN(PHIL)/Y(4)
    THETA=57.3*(Y(1)+Y(2))

```

C *****VARIABLES ARE CHANGED TO DEGREES FOR PRINT OUT*****

```

OMTP=57.3*OMT
OMLP=57.3*OML
OMRP=57.3*OMR
PHITP=57.3*PHIT
PHILP=57.3*PHIL
LAVP=57.3*Y(5)
LAMT=57.3*Y(1)

```

SRMT

TRACE

CDC 6400 FTN V3.0-P336 OPT=1 04/13/73

LAML=57.3*Y(2)

KD=KD+1

IF(KD-5) 511,508,508

508 KD=0

PRINT 510,T,PHITP,NT,Y(7),LAMT,LAML,THETA,NL,PHILP,OMLP,Y(4),Y(3),
10MRP,LAVP

510 FORMAT(2X,F5.2,2X,F5.2,2X,F5.2,2X,F8.1,1X,F7.2,2X,F7.2,2X,F7.2,2X,
1F6.2,2X,F7.2,2X,F8.2,1X,F8.1,2X,F8.1,1X,F8.2,2X,F8.6)

511 K=K+1

IF(T-25) 514,1,1

514 IF(K-270) 200,515,515

515 PRINT 516

516 FORMAT(1H1//* TIME PHII TAR-G I-VEL LAM-I LAM-L I
1HETA LAU-G PHIL OMEG-L L-VEL RANGE OMEG-R LAM
2-V*)

K=0

GOTO 200

520 STOP

END

SAMPLE COMPUTER OUTPUT

THE INPUT VARIABLES ARE		Printout Parameter	Definition	Symbol
W= 30000.		PHIT	bank angle of the target	ϕ_T
S= 530.00		TAR-G	target load factor	n_T
CL= 2.2300		T-VEL	target true velocity	V_T
CDZ= .0150		LAM-T	angle between target velocity vector and line of sight	λ_T
AR= 2.7300		LAM-L	angle between launcher velocity vector and line of sight vector	λ_L
EP= .9000		THETA	track crossing angle	TCA, θ
TAU= 1.0000		LAU-G	launcher load factor	n_L
RO= .00200		PHIL	bank angle of the launcher	ϕ_L
VL= .550.00		OMEG-L	angular rate of launcher velocity vector	ω_L
VT= 850.00		L-VEL	launcher true velocity	V_L
RZ= 3000.0		RANGE	range	R
DEL= .0350		OMEG-R	angular rate of line of sight vector	ω_R
NC= 4.0000		LAM-V	angle between line of sight and the horizontal plane adjacent to the launcher	λ_V
CLAT= 4.5000				
WD= 1300.				
CD70= .0150				
VZ= 325.00				
VZT= 850.00				

TIME	PHIT	TAR-G	T-VEL	LAM-T	LAM-L	THETA	LAU-G	PHIL	OMEG-L	L-VEL	RANGE	OMEG-R	LAM-V
0.00	0.00	1.00	850.0	1.00	-0.04	-0.00	1.02	10.03	.38	850.0	3000.0	-0.01	-0.245057
.50	62.71	2.14	849.9	1.04	-0.05	1.02	1.19	-52.01	-2.03	850.4	2999.9	.23	0.049442
1.00	69.81	2.30	849.4	1.24	.00	7.37	1.25	25.12	1.15	850.8	2999.2	.95	.170945
1.50	72.93	3.38	848.6	5.84	.16	5.99	1.32	29.45	1.41	851.2	2996.7	1.69	.276686
2.00	73.85	3.59	847.6	4.42	.32	8.75	1.42	41.81	2.05	851.5	2991.8	2.47	.363148
2.50	74.96	3.75	846.5	10.27	.56	11.44	1.55	52.19	2.65	851.7	2983.5	3.23	.437826
3.00	74.95	3.85	845.7	17.11	.84	13.39	1.73	59.51	3.23	851.9	2971.3	3.95	.513237
3.50	75.14	3.91	844.1	15.04	1.27	16.15	1.95	63.94	3.79	851.9	2955.0	4.62	.619061
4.00	75.32	3.95	842.8	15.80	1.70	18.49	2.20	66.30	4.36	851.8	2934.6	5.25	.744539
4.50	75.40	3.97	841.5	19.25	2.14	20.39	2.46	67.40	4.93	851.4	2918.5	5.81	.880607
5.00	75.45	3.98	840.2	19.45	2.58	22.03	2.72	67.83	5.47	850.8	2903.1	6.32	1.049667
5.50	75.48	3.99	838.9	20.44	2.99	23.43	2.97	67.97	5.98	849.9	2888.0	6.77	1.249662
6.00	75.50	3.99	837.6	21.22	3.38	24.59	3.20	68.09	6.45	849.7	2872.7	7.17	1.486887
6.50	75.51	4.00	836.3	21.82	3.73	25.55	3.39	68.15	6.87	849.2	2866.7	7.53	1.747921
7.00	75.52	4.00	835.0	22.27	4.04	26.30	3.56	68.15	7.25	848.5	2851.8	7.83	2.036139
7.50	75.52	4.00	833.7	22.57	4.32	26.89	3.70	68.05	7.58	848.5	2836.2	8.09	2.359792
8.00	75.52	4.00	832.4	22.77	4.56	27.33	3.80	70.75	7.87	848.3	2820.6	8.32	2.709233
8.50	75.53	4.00	831.1	22.86	4.77	27.63	3.88	72.13	8.13	848.0	2805.2	8.51	3.086607
9.00	75.53	4.00	829.8	22.88	4.95	27.83	3.94	73.71	8.34	847.5	2790.4	8.67	3.494388
9.50	75.53	4.00	828.4	22.82	5.10	27.93	3.98	75.18	8.52	847.0	2776.5	8.80	3.929972
10.00	75.53	4.00	827.3	22.77	5.23	27.95	4.01	76.98	8.67	846.3	2763.5	8.91	4.393257
10.50	75.53	4.00	826.0	22.57	5.35	27.91	4.03	78.36	8.79	846.0	2751.0	8.99	4.880683
11.00	75.53	4.00	824.8	22.38	5.44	27.83	4.05	79.36	8.88	845.9	2740.3	9.06	5.382448
11.50	75.53	4.00	823.5	22.17	5.53	27.70	4.06	79.88	8.96	845.1	2730.3	9.12	5.888820
12.00	75.53	4.00	822.3	21.95	5.60	27.55	4.07	79.85	9.02	845.3	2720.7	9.16	6.400237
12.50	75.53	4.00	821.0	21.71	5.67	27.38	4.09	79.25	9.05	845.6	2708.5	9.19	6.925258
13.00	75.53	4.00	819.8	21.47	5.73	27.20	4.10	78.25	9.09	845.6	2694.0	9.21	7.463671
13.50	75.53	4.00	818.5	21.22	5.79	27.01	4.12	76.91	9.11	845.7	2678.9	9.22	8.018037
14.00	75.53	4.00	817.3	20.98	5.84	26.82	4.13	75.44	9.13	845.8	2663.4	9.22	8.584628
14.50	75.53	4.00	816.1	20.74	5.89	26.63	4.15	74.03	9.13	845.8	2649.5	9.22	9.161540
15.00	75.53	4.00	814.9	20.51	5.93	26.44	4.16	72.68	9.14	845.7	2636.1	9.22	9.748829
15.50	75.53	4.00	813.6	20.29	5.97	26.26	4.16	72.11	9.14	845.7	2624.3	9.21	1.023421
16.00	75.53	4.00	812.4	20.08	6.00	26.09	4.15	71.42	9.14	845.6	2613.9	9.19	1.0967650
16.50	75.53	4.00	811.2	19.89	6.03	25.92	4.13	72.04	9.13	845.5	2605.1	9.18	1.1951063
17.00	75.53	4.00	810.0	19.71	6.05	25.76	4.10	72.73	9.13	845.5	2598.6	9.15	1.276271
17.50	75.53	4.00	808.8	19.55	6.06	25.61	4.05	73.33	9.12	845.5	2592.5	9.13	1.3753719
18.00	75.53	4.00	807.6	19.41	6.04	25.48	4.00	75.18	9.10	845.6	2581.7	9.10	1.4600401
18.50	75.53	4.00	806.4	19.29	6.06	25.35	3.96	76.63	9.08	845.7	2570.0	9.08	1.5437698
19.00	75.53	4.00	805.2	19.19	6.06	25.25	3.91	77.97	9.06	845.0	2558.4	9.06	1.628569
19.50	75.53	4.00	804.0	19.11	6.06	25.16	3.87	79.01	9.04	845.3	2548.8	9.04	1.714493
20.00	75.53	4.00	802.9	19.04	6.06	25.10	3.84	79.58	9.01	845.7	2540.1	9.02	1.802563
20.50	75.53	4.00	801.7	18.99	6.06	25.05	3.82	79.98	8.99	845.1	2532.3	9.00	1.893161
21.00	75.53	4.00	800.5	18.95	6.07	25.02	3.80	79.00	8.97	845.6	2524.4	8.99	1.976430
21.50	75.53	4.00	799.3	18.92	6.09	25.01	3.80	77.91	8.95	845.0	2517.2	8.99	2.0632173
22.00	75.53	4.00	798.2	18.90	6.11	25.01	3.80	76.45	8.93	845.5	2510.8	8.98	2.1530510
22.50	75.53	4.00	797.0	18.89	6.14	25.03	3.81	74.81	8.91	845.0	2507.2	8.98	2.2463067
23.00	75.53	4.00	795.9	18.89	6.17	25.06	3.82	73.21	8.90	845.4	2506.3	8.98	2.3435985
23.50	75.53	4.00	794.7	18.89	6.21	25.10	3.84	71.83	8.90	845.8	2506.2	8.97	2.4448884
24.00	75.53	4.00	793.4	18.90	6.25	25.15	3.84	70.82	8.89	845.1	2506.9	8.97	2.549754
24.50	75.53	4.00	792.4	18.92	6.29	25.21	3.84	70.28	8.90	845.4	2508.4	8.97	2.649377
25.00	75.53	4.00	791.3	18.95	6.32	25.27	3.83	70.24	8.92	845.7	2510.6	8.96	2.745823

REFERENCES

1. AIM and Preprogrammed Modes for the Versatile Automatic Flight Control System in the BQM-34A (A/A 376-8 AFCS), Lear-Seigler, Inc., Astronics Division, Los Angeles, California, 18 December 1972.
2. Improved Increased Maneuverability, MDC-TR-68-45, Air Force Missile Development Center, Holloman AFB, New Mexico, May 1968.

UNCLASSIFIED

Security Classification

DOCUMENT CONTROL DATA - R & D

(Security classification of title, body of abstract and indexing annotation must be entered when the overall report is classified)

1. ORIGINATING ACTIVITY (Corporate author)

Air Force Flight Test Center
Edwards AFB, California

2a. REPORT SECURITY CLASSIFICATION

Unclassified

2b. GROUP

N/A

3. REPORT TITLE

Determining the Performance Envelopes of Short Range Missiles

4. REPORT TYPE AND DATES COVERED

Final Report Feb 69 - Nov 72

5. AUTHOR (Last name, first name, middle initial, last name)

Thomas P. McAtee Major USAF

6. REPORT DATE

October 1973

47

7b. NO. OF REFS

2

8a. CONTRACT OR GRANT NO.

b. PROJECT NO.

N/A

d.

9a. ORIGINATOR'S REPORT NUMBER(S)

AFTC-TD-73-4

9b. OTHER REPORT NO(S) (Any other numbers that may be assigned this report)

N/A

10. DISTRIBUTION STATEMENT

Distribution limited to U.S. Government agencies only (Test and Evaluation), August 1973. Other requests for this document must be referred to AFTC (DOFC), Edwards AFB, California 93523.

11. SUPPLEMENTARY NOTES

N/A

12. SPONSORING MILITARY ACTIVITY

Deputy Commander for Operations
Air Force Flight Test Center
Edwards AFB, California

13. ABSTRACT

➤ This report presents the results of a study to develop a reliable test method for determining a short range missile's performance envelope. Three main areas are covered: (1) drone control; (2) derivation of a computer program for predicting flightpath relationships; and (3) a new test technique that, when properly applied, will guarantee that the missile is launched on the edge of its envelope. This technique is unique in that it allows the missile to be fired at a number of acceptable launch conditions and uses real time computation to determine when an acceptable launch condition exists. Application of this method is simple and inexpensive. Added to that, its inherent reliability will allow test agencies to accurately determine a missile's performance envelope and will result in substantial savings by greatly reducing the number of required missile launches for envelope determination.

UNCLASSIFIED
Security Classification

14.	KEY WORDS	LINK A		LINK B		LINK C	
		ROLE	WT	ROLE	WT	ROLE	WT
missile performance drones computers launch conditions missile testing							

UNCLASSIFIED
Security Classification